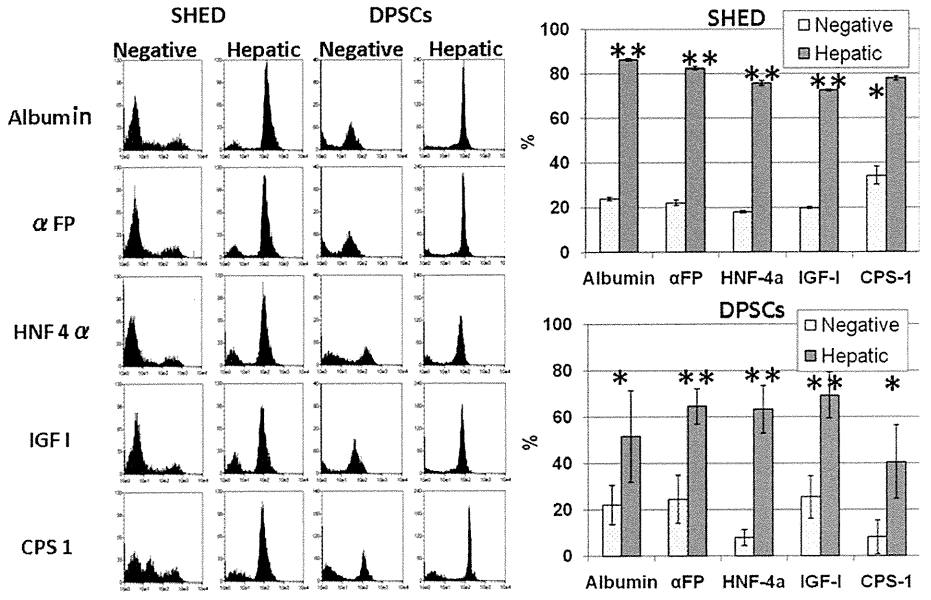

Figure 5. Flow cytometric analysis. Left: typical histograms of albumin, α-FP, HNF-4α, IGF-1, and CPS-1, detected by using Alexa Fluor 568 as secondary antibody (n = 5, respectively). Right: percentage of cells positive for α-FP, HNF-4α, IGF-1, and CPS-1 after 20 days of differentiation following the differentiation protocol. High purity of hepatic cells was observed. Nondifferentiated cells were fluorescently marked with the same antibodies and were used as negative controls. *P < .001; **P < .0001.

medium from SHED (Fig. 6). Fresh medium with additives used as a negative control showed no presence of urea.

Discussion

The present study demonstrates that the CD117-positive fractions of SHED and DPSCs are differentiated into morphologic and functional hepatocyte-like cells in serum-free conditions *in vitro*. In the past, several studies have focused on the adult stem cells in dental structures (18–20). Cell cultures from deciduous and extracted third molar pulp, periodontal ligaments, and tooth germs have been isolated and characterized. Most scientists' efforts in dental stem cells were concentrated on differentiating the cells to tissues related to their specialty, ie, dentistry. The cells were differentiated into odontogenic, osteogenic, periodontal lineages (21–23), etc. We found that the immunologic characterization of the CD117-positive fractions showed expression of stem cell markers associated with all 3 germ layer predecessor cells, including CK19, nestin, and Oct 3/4, markers associated with hepatoblasts (24–26). Even after 70 population doublings by using magnetic separation every 4 passages, the fraction showed similar characteristics as the above (data not shown). It was suggested that it is possible to produce huge numbers of stem cell fractions by using CD117 magnetic separation.

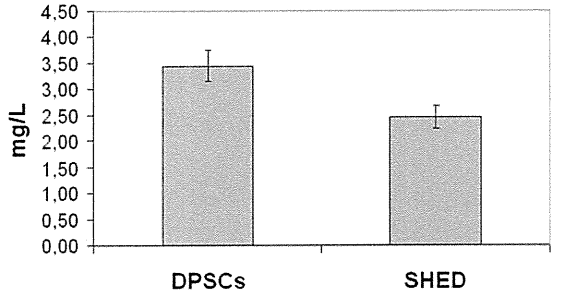

Figure 6. Concentration of urea in the culture medium. Three days before the end of the differentiation protocol, the medium was replaced with fresh medium. Culture medium was collected on the last day of the protocol and analyzed colorimetrically (n = 5). Fresh medium with additives was used as a negative control, P < .0001.

In our previous study, we differentiated SHED and DPSCs into an embryologically distant lineage such as a hepatic lineage (1). In the embryogenesis, growth factors and cytokines such as HGF and oncostatin M play crucial role in guiding the hepatogenesis. The importance of HGF for hepatic development and regeneration is well described (27, 28). Oncostatin M is a member of the interleukin-6 family and has been proved to play a leading role in guiding hepatoblasts toward maturation (29, 30). SHED or DPSCs were differentiated in SFM with these 2 compounds and changed their morphology from spindle-shaped fibroblast-like cells to ovoid hepatocyte-like cells. After 28 days of differentiation and maturation the cells expressed markers related to hepatocytes: albumin, αFP, IGF-I, HGF-4α, and CPS-1.

We were aware that the use of animal products during the period of differentiation might present occult qualities and complications for any future clinical application of the differentiated lineages of SHED or DPSCs. To minimize the effect of serum on the cells, we used an SFM that we previously designed for culturing SHED and DPSCs, although proliferation rates of SHED and DRSC were found to be 35%–55% compared with DMEM containing 10% FBS (13). DMEM with 10% FBS was used only for the first day after every passage. On the second day after passage, the medium was quickly replaced with SFM. Moreover, SFM was used at every step for differentiation.

By this means we could increase the palette of possible clinical applications of dental stem cell lineages. Our protocol in this study might be acceptable for future clinical applications in regenerative medicine that use SHED or DPSCs.

We found that the number of positive cells to each 5 hepatic markers was 70%–90% in SHED and 40%–70% in DPSCs. This suggests that transplantation studies in animals or humans might become practical in the near future. However, a difference in the markers' expression was found between SHED and DPSCs. SHED also demonstrated similar characteristics in neurogenic differentiation to that demonstrated by bone marrow mesenchymal stem cells (22). Furthermore,

Huang et al (31) described that SHED represent a population of multipotent stem cells that might be more immature than other postnatal stromal stem cell populations. Our results suggest that SHED might be a better hepatic progenitor source than DPSCs are.

Embryonic stem cells and induced pluripotent stem cells frequently cause teratoma and/or other tumors after transplantation into animals (32, 33). Preventing tumor formation is essential for future regenerative medicine and yet extremely difficult. In contrast with embryonic stem cells or induced pluripotent stem cells, it was reported that when undifferentiated bone marrow stem cells were even directly transplanted into animals and humans, teratoma has not yet been found. Therefore, Jiang et al (34) emphasized that the systemic use of undifferentiated bone marrow stem cells might be allowed. However, the possibility that stromal stem cells produce tumors was described (2, 35). It is implied that transplantation of differentiated cells from stromal stem cells might have less possibility of producing tumors than stem cell transplantation, because the protocol is similar to organ transplantations and because differentiated cells are transplanted. Moreover, transplantation of the differentiated cells containing less contamination of undifferentiated cells (in the above case) might have much less probability to cause neoplasms. Our results showed that most of the cells in the CD117-positive fraction were differentiated into high-purity hepatic lineages, ie, the ratio of albumin-positive cells was almost 90% in SHED. Hence, the fractionation of CD117-positive cells might allow us to differentiate the cells into hepatogenic lineage for future transplantations.

Acknowledgments

The authors deny any conflicts of interest related to this study.

References

1. Ishkitiev N, Yaegaki K, Calenic B, et al. Deciduous and permanent dental pulp mesenchymal cells acquire hepatic morphological and functional features in vitro. J Endod 2010;36:469–74.
2. Joachim DH, Socié G. Malignancies after hematopoietic stem cell transplantation: many questions, some answers. Blood 1998;91:1833–44.
3. Taléns-Visconti R, Bonora A, Jover R, et al. Hepatogenic differentiation of human mesenchymal stem cells from adipose tissue in comparison with bone marrow mesenchymal stem cells. World J Gastroenterol 2006;12:5834–45.
4. Jin L, Ji S, Wang X, Guo X, Chen H, Ji W. Hepatocytic differentiation of rhesus monkey embryonic stem cells promoted by collagen gells and growth factors. Cell Biol Int 2011;35:775–81.
5. Marongiu F, Gramignoli R, Dorko K, et al. Hepatic differentiation of amniotic epithelial cells. Hepatology 2011;53:1719–29.
6. Chen Y, Zhou H, Sarver AL, et al. Hepatic differentiation of liver-derived progenitor cells and their characterization by microRNA analysis. Liver Transpl 2010;16: 1086–97.
7. Agarwal S, Holton KL, Lanza R. Efficient differentiation of functional hepatocytes from human embryonic stem cells. Stem Cells 2008;26:1117–27.
8. Miettinen M, Lasota J. A review on expression in normal and neoplastic tissues, and mutations and their clinicopathologic correlation. Appl Immunohisto M M 2005;13: 205–20.
9. Said T, Agarwal A, Zborowski M, Grunewald S, Glander H, Paasch U. Utility of magnetic cell separation as a molecular sperm preparation technique. J Androl 2008;29:134–42.
10. Calenic B, Ishkitiev N, Yaegaki K, et al. Magnetic separation and characterization of keratinocyte stem cells from human gingiva. J Periodont Res 2010;45:703–8.
11. Kobayashi C, Yaegaki K, Calenic B, et al. Hydrogen sulfide causes apoptosis in human pulp stem cells. J Endod 2011;37:479–84.
12. Kuznetsov SA, Mankani MH, Robey PG. Effect of serum on human bone marrow stromal cells: ex vivo expansion and in vivo bone formation. Transplantation 2000;70:1780–7.
13. Hirata TM, Ishkitiev N, Yaegaki K, et al. Expression of multiple stem-cell markers in dental-pulp cells cultured in serum-free media. J Endod 2010;36:1139–44.
14. Morito A, Kida Y, Suzuki K, et al. Effects of basic fibroblast growth factor on the development of the stem cell properties of human dental pulp cells. Arch Histol Cytol 2009;72:51–64.
15. Ishiwata I, Tokieda Y, Kiguchi K, Sato K, Ishikawa H. Effects of embryotrophic factors on the embryogenesis and organogenesis of mouse embryos in vitro. Hum Cell 2000;13:185–95.
16. Jackson MJ, Beaudet AL, O'Brien WE. Mammalian urea cycle enzymes. Annu Rev Genet 1986;20:431–64.
17. Sesti S, Martino G, Mazzulla S, Chimenti R. Effect of bradykinin on nitric oxide production, urea synthesis and viability of rat hepatocyte cultures. BMC Physiol 2005;5:2.
18. Suzuki T, Lee CH, Chen M, et al. Induced migration of dental pulp stem cells for in vivo pulp regeneration. J Dent Res 2011;90:1013–8.
19. Mori G, Brunetti G, Oranger A, Carbone C, Ballini A, Lo Muzio L, Colucci S, Mori C, Grassi FR, Grano M. Dental pulp stem cells: osteogenic differentiation and gene expression. Ann N Y Acad Sci 2011;1237:47–52.
20. Rodriguez-Lozano FJ, Bueno C, Insausti CL, et al. Mesenchymal stem cells derived from dental tissues. Int Endod J 2011;44:800–6.
21. Gronthos S, Mankani M, Brahim J, Robey PG, Shi S. Postnatal human dental pulp stem cells (DPSCs) in vitro and in vivo. Proc Natl Acad Sci U S A 2000;97: 13625–30.
22. Miura M, Gronthos S, Zhao M, et al. SHED: stem cells from human exfoliated deciduous teeth. Proc Natl Acad Sci U S A 2003;100:5807–12.
23. Guven EP, Yalvac ME, Sahin F, Yazici MM, Rizvanov AA, Bayirli G. Effect of dental materials calcium hydroxide–containing cement, mineral trioxide aggregate, and enamel matrix derivative on proliferation and differentiation of human tooth germ stem cells. J Endod 2011;37:650–6.
24. Friedman SL. The virtuosity of hepatic stellate cells. Gastroenterology 1999;117: 1244–6.
25. Yamada Y, Nishimoto E, Mitsuya H, Yonemura Y. In vitro transdifferentiation of adult bone marrow Sca-1+ cKit- cells cocultured with fetal liver cells into hepatic-like cells without fusion. Exp Hematol 2006;34:97–106.
26. Thenappan A, Li Y, Kitisin K, et al. Role of transforming growth factor β signaling and expansion of progenitor cells in regenerating liver. Hepatology 2010;51:1373–82.
27. Fausto N, Campbell JS, Riehle KJ. Liver regeneration. Hepatology 2006;43:S45–53.
28. Duncan AW, Dorrell C, Grompe M. Stem cells and liver regeneration. Gastroenterology 2009;137:466–81.
29. Miyajima A, Kinoshita T, Tanaka M, Kamiya A, Mukouyama Y, Hara T. Role of oncostatin M in hematopoiesis and liver development. Cytokine Growth Factor Rev 2000;11:177–83.
30. Hamazaki T, Iiboshi Y, Oka M, et al. Hepatic maturation in differentiating embryonic stem cells in vitro. FEBS Lett 2001;497:15–9.
31. Huang GT, Gronthos S, Shi S. Mesenchymal stem cells derived from dental tissues vs those from other sources: their biology and role in regenerative medicine. J Dent Res 2009;88:792–806.
32. Brederlau A, Correia AS, Anisimov SV, et al. Transplantation of human embryonic stem cell-derived cells to a rat model of Parkinson's disease: effect of in vitro differentiation on graft survival and teratoma formation. Stem Cells 2006;24:1433–40.
33. Takahashi K, Tanabe K, Ohnuki M, et al. Induction of pluripotent stem cells from adult human fibroblasts by defined factors. Cell 2007;131:861–72.
34. Jiang Y, Jahagirdar BN, Reinhardt RL, et al. Pluripotency of mesenchymal stem cells derived from adult marrow. Nature 2002;418:41–9.
35. Bianco P, Riminucci M, Gronthos S, Robey PG. Bone marrow stromal stem cells: nature, biology, and potential applications. Stem Cells 2001;19:180–92.

Journal of
PERIODONTAL RESEARCH

J Periodont Res 2012; 47: 365–373

JOURNAL OF PERIODONTAL RESEARCH
doi:10.1111/j.1600-0765.2011.01442.x

Oral malodorous compound causes caspase-8 and -9 mediated programmed cell death in osteoblasts

I. Aoyama, B. Calenic, T. Imai, H. Ii, K. Yaegaki
Department of Oral Health, The Nippon Dental University, Tokyo, Japan

Aoyama I, Calenic B, Imai T, Ii H, Yaegaki K. Oral malodorous compound causes caspase-8 and -9 mediated programmed cell death in osteoblasts. J Periodont Res 2012; 47: 365–373. © 2011 John Wiley & Sons A/S

Background and Objective: Hydrogen sulfide (H_2S) is one of two volatile sulfur compounds that are known to be the main cause of oral malodor; the other is methyl mercaptan. Other known volatiles existing in mouth air do not contribute significantly to oral malodor originating in the oral cavity. Hydrogen sulfide is also known to be an etiological factor in periodontal disease. However, the effects of H_2S on alveolar bone remain unclear. The objectives of this study were to determine the apoptotic effects of H_2S on osteoblasts and to verify the apoptotic molecular pathways.

Material and Methods: A clonal murine calvaria cell line was incubated with 50 ng/mL of H_2S. To detect apoptosis, the cells were analysed by flow cytometry and ELISA. Mitochondrial membrane depolarization was assessed using flow cytometry as well. ELISA was used to evaluate the release of cytochrome *c* into the cytosol and to assess Fas ligand, p53, tumor necrosis factor α, interleukin IL1-α IL-β, IL-2, IL-4, IL-10, interferon-γ, granulocyte-colony stimulating factor and granulocyte-macrophage colony stimulating factor. Caspase-3, -8 and -9 activities were estimated. Expression of *BAX* and *Bcl-2* was assessed by real-time quantitative RT-PCR. DNA fragmentation was detected by single-cell gel electrophoresis. Fas receptors were evaluated by western blotting.

Results: After H_2S incubation, apoptotic levels increased significantly in a time-dependent manner. Mitochondrial membrane depolarization, the release of cytochrome *c*, p53 and caspase-3, -8 and -9 and DNA fragmentation were all significantly greater. *BAX* gene activity was upregulated, whereas *Bcl-2* remained low. Fas ligand/Fas receptor, tumor necrosis factor α and other cytokines were not increased to a significant degree.

Conclusion: At less-than-pathological concentrations in gingival crevicular fluid, H_2S induces apoptosis in osteoblasts. The molecular mechanisms underlying the apoptotic process include p53, a mitochondrial pathway and caspase-8 activation.

Ken Yaegaki, DDS, PhD, Department of Oral Health, Nippon Dental University, 1-9-20 Fujimi, Chiyoda-ku, Tokyo 102-8159, Japan
Tel: +81 3 3261 8791
Fax: +81 3 3261 8796
e-mail: yaegaki-k@tky.ndu.ac.jp

Key words: apoptosis; halitosis; osteoblast; periodontitis

Accepted for publication October 16, 2011

Volatile sulfur compounds (VSCs), specifically hydrogen sulfide (H_2S) and methyl mercaptan (CH_3SH), have been shown to cause halitosis and also to correlate with the strength of oral malodor (1). Van den Velde *et al.* (1) demonstrated that H_2S and CH_3SH alone significantly contribute to oral malodor originating from the oral cavity and that the role of other compounds found in mouth air is insignificant. Indeed, H_2S is always present in both physiological

and oral pathological halitosis (2). Previous studies, variously employing gas chromatography, portable gas chromatography or a chemical procedure, have demonstrated a clear relationship among the concentration of VSCs, periodontal disease and periodontal pathogens (3–11). The few papers that failed to demonstrate this relationship utilized a portable sulfide monitor for detecting H_2S (12,13).

Some VSCs are known to be highly toxic. Hydrogen sulfide inhibits cytochrome *c* oxidase via a mechanism similar to that of hydrogen cyanide; consequently, H_2S causes death by means of cellular asphyxiation (14,15). Volatile sulfur compounds have also been shown to comprise one of the pathogenic factors involved in periodontitis (16). Volatile sulfur compounds, particularly H_2S, induce the differentiation of osteoclasts in alveolar bone (17). Moreover, increased levels of VSCs both strongly suppress the synthesis of collagen and increase collagen degradation in human gingival fibroblasts (18,19). Furthermore, VSCs obstruct the normal functioning of the basement membrane by making the mucosa more permeable to periodontitis-causing agents, such as lipopolysaccharides and prostaglandin E_2 (20). Recent studies have described the activation of apoptosis by H_2S in human gingival soft tissues, such as fibroblasts, keratinocytes and keratinocyte stem cells (21–23).

Alveolar bone loss is one of the key events in the development of periodontitis, resulting in part from increased osteoclast resorption and/or decreased osteoblast formation. Some growth factors and inflammatory cytokines affect the development of both osteoclasts and osteoblasts (24). Tumor necrosis factor α (TNF-α) and interleukin 1β (IL-1β) can induce apoptosis in mouse osteoblasts (25). Hydrogen sulfide easily diffuses through the oral mucosa of a gingival crevice model (20) and causes pathological changes of alveolar bone tissues in an *in vivo* rat model (17). *In vitro* studies have shown that it also causes inhibition of osteoblast proliferation (26) and induction of osteoclast differentiation (27). We previously reported that H_2S causes apoptosis in some oral tissues (21–23). However, as H_2S causes either apoptotic or anti-apoptotic activities in different tissues (28–30), H_2S could have an anti-apoptotic effect on osteoblasts.

The objectives of the present study were to determine whether H_2S causes apoptosis in osteoblasts, as it has been shown to do in other oral tissues (21–23) and, if so, to identify these apoptotic molecular pathways.

Material and methods

Cell culture

The osteoblastic cell line MC3T3-E1, derived from newborn mouse calvaria, was employed in this study (26). The cells were cultured in α-minimum essential medium (Gibco, Grand Island, NY, USA) enriched with 10% fetal bovine serum (Hyclone, Logan, UT, USA) and 5 μg/mL gentamicin (Gibco) at 37°C in an atmosphere of air containing 5% CO_2. For each independent experiment, 5×10^5 cells were cultured in 25 cm^2 flasks and allowed to attach overnight. Before their incubation with H_2S, the cells were placed in fresh medium.

Hydrogen sulfide incubation system

The cells were incubated in enriched medium in a chamber infused at approximately 200 mL/min with a constant flow of humidified air containing 5% CO_2 mixed with 50 ng/mL of H_2S for 24, 36 and 48 h, as described previously (21–23), following the procedures of Yaegaki *et al.* (21). Permeator (Gastec, Kanagawa, Japan) and H_2S permeation tubes (Gastec) were used to produce a 50 ng/mL concentration of H_2S in the test chamber. As a result of diffusion, the H_2S concentration in the medium was measured as 18 ng/mL (0.5 μM), much lower than that found in gingival crevicular fluids from periodontal gingival tissues (31). Healthier gingiva showed lower concentrations (31), so the concentration of H_2S was less than that found in pathological conditions. Control cultures were incubated in 5% CO_2 and 95% air for 24, 36 and 48 h.

Detection of early apoptosis

Apoptotic and nonapoptotic cells were detected using Guava Nexin PCA (GE Healthcare Bioscience, Tokyo, Japan) flow cytometric analysis. Briefly, the cells were stained with two fluorescent dyes: annexin V and 7-amino actinomycin D (7-AAD). Annexin V binds to phosphatidylserine at the cell surface during the early stages of apoptosis and dyes the apoptotic cells, while 7-AAD penetrates the cell membrane only at the later stages of apoptosis or necrosis and binds to DNA. After H_2S incubation, the cells were washed with phosphate-buffered saline (PBS) solution and trypsinized. Pellet (cells fraction), medium and PBS for washing were collected and then resuspended in cold Guava Nexin buffer at 1×10^6 cells/mL, followed by staining as described above. The samples were analysed using Guava EasyCyte and Guava CytoSoft software (Guava Technologies, Hayward, CA, USA).

To distinguish clearly between apoptosis and necrosis, the cells were also analysed with Cell Death Detection ELISA Plus (Roche Applied Science, Mannheim, Germany) according to the manufacturer's instructions. This assay quantifies histone-complexed DNA fragments, i.e. mono- and oligonucleosomes, in apoptotic cells. After H_2S treatment, the cells were washed with PBS, trypsinized and pelleted, thus removing DNA originating from necrotic cells in the supernatant. The pellet was resuspended in lysis buffer at a concentration of 5×10^4 cells/mL. After lysis, the supernatant containing histone-complexed DNA fragments was added to a streptavidin-coated microplate for analysis. Peroxidase-labeled anti-DNA antibody binds to the histone-complexed DNA fragments of nucleosomes. After unbound antibodies had been flushed out, the amount of nucleosome material present was measured as peroxidase activity included in the immune complex. The amount of peroxidase was measured with 2,2′-azino-di[3-ethylbenzthiazolinsulfonate] as a substrate, and the microplate reader (Bio-Rad Benchmark; Bio-Rad Japan, Tokyo, Japan) was set to 405 nm, with a wavelength correction set to 490 nm.

An enrichment factor (EF) showing the specific enrichment of mono- and oligonucleosomes released into the cytoplasm was derived by dividing the absorbance value (AV) of the sample by the AV of the negative control.

Detection of mitochondrial membrane potential

Guava EasyCyte MitoPotential Kit (Guava Technologies) was used to detect depolarization of the mitochondrial membrane potential. This assay employs two fluorescent dyes: 5,5′,6,6′-terachloro-1,1′,3,3′-tetra ethyl benzimidazole carbocyanine iodide (JC-1), for evaluating the mitochondrial membrane potential changes, and 7-AAD for indicating late-stage apoptotic and necrotic cells. After H_2S exposure, the cells were washed with PBS, trypsinized and centrifuged. They were resuspended in 200 μL of medium at a final concentration of 5×10^5 cells/mL, followed by the addition of 2 μL of JC-1 and 2 μL of 7-AAD. After 30 min incubation at 37°C in air containing 5% CO_2, the cells were analysed by means of flow cytometry (Guava EasyCyte; Guava Technologies).

Detection of cytochrome *c*

Rat/mouse cytochrome *c* immunoassay (R&D Systems, Minneapolis, MN, USA) was used for cytochrome *c* detection. The cells were washed three times with PBS to remove serum components and then permeabilized using PBS containing 0.5% Triton X-100 at a concentration of 1×10^6 cells/mL. Following centrifugation, the supernatant, the cytosolic fraction, was added to the wells together with an enzyme-linked monoclonal antibody specific for cytochrome *c*. After the unbound antibodies were washed out, a substrate solution was added to each well according to the manufacturer's instructions. The color developed in proportion to the amount of cytochrome *c* available in each sample. The optical density was measured using a microplate reader (Bio-Rad Benchmark; Bio-Rad Japan) set to 450 nm, with a wavelength correction set to 540 nm.

Detection of caspase-3, -8 and -9 activity

Specific detection kits were employed for the quantitative assessment of caspase-3, -8 and -9 (Calbiochem, San Diego, CA, USA). The assays involve nontoxic and cell-permeable fluorescent markers that bind irreversibly to activated caspase-3, -8 or -9. Briefly, 300 μL of each sample, concentrated at 1×10^6 cells/mL, was labeled with 1 μL of fluorescein isothiocyanate fluorescein-conjugated Asp-Glu-Val-Asp-O-methyl-fluormethylketon for caspase-3, fluorescein-conjugated Ile-Glu(OMe)-Thr-Asp-O-methyl-fluormethylketon for caspase-8 or fluorescein-conjugated Leu-Glu(OMe)-His-Asp-O-methyl-fluormethylketon for caspase-9. After 1 h of incubation at 37°C, the FITC label allowed direct detection of each activated caspase with a fluorescence plate reader (Fluoroskan Ascent FL, Vantaa, Finland). The samples were measured at excitation filter = 485 nm and emission filter = 535 nm.

Detection of p53

The p53 pan ELISA kit (Roche Applied Science) was used to detect the tumor-suppressor protein p53, which triggers both mitochondrial pathways and cell-death ligand/receptor pathways involving caspase-8 (32–36). After H_2S incubation, the cells were washed with PBS, trypsinized, pelleted, and resuspended in lysis buffer at a concentration of 1×10^7 cells/mL. Standards, samples or controls were pipetted into wells precoated with the biotin-labeled capture antibody. The p53-containing sample reacts with captured antibody and peroxidase-labeled detection antibody to form a stable immunocomplex. Subsequent to the washing step, the peroxidase bound in the complex is developed by tetramethylbenzidine as a substrate. Assay results are quantified spectrophotometrically at 450 nm, with a correction wavelength of 690 nm using a microtiter plate reader (Bio-Rad Benchmark; Bio-Rad Japan).

Real-time quantitative RT-PCR

Real-time quantitative RT-PCR was used to analyse the levels of pro-apoptotic (*BAX*) and anti-apoptotic (*Bcl-2*) gene expression. The cells were seeded in enriched medium in 96-well plates at a concentration of 1×10^5 cells/mL and then incubated with or without 50 ng/mL H_2S for 24, 36 or 48 h. TaqMan Gene Expression Cells-to-CT Kit™ (Ambion®, Austin, TX, USA) was used according to the manufacturer's instructions for all steps from isolation of RNA to RT-PCR. To extract RNA, the cells were washed with PBS and treated with lysis solution containing Dnase I. The lysates were used as a template for the synthesis of cDNA. The RT reaction was carried out for 1 h at 37°C followed by 5 min at 95°C. Real-time quantitative RT-PCR (StepOnePlus Real-Time PCR System; Applied Biosystems, Foster City, CA, USA) was performed in the following conditions: 2 min at 50°C, 10 min at 95°C, followed by 40 cycles of 15 s at 95°C, and 1 min at 60°C. β-Actin was used as an endogenous control. Each sample was analysed in triplicate. The levels of the relative quantification were calculated by StepOne Software version 2.0 (StepOnePlus Real-Time PCR System; Applied Biosystems) using the $2^{-\Delta\Delta C_T}$ method (37).

DNA fragmentation

Single-cell gel electrophoresis (Comet Assay; Trevigen, Gaithersburg, MD, USA) was used to detect genomic DNA fragmentation. This assay exploits the capacity of cleaved DNA fragments to migrate out of the nucleoid under the influence of an electric field. Undamaged DNA migrates more slowly than damaged DNA or remains within the confines of the nucleoid. Viewed under the microscope, the cell is comet shaped, with its head corresponding to the nuclear region and its tail showing the damaged DNA fragments.

The cells were suspended in PBS at a concentration of 1×10^5 cells/mL. After cell lysis was accomplished with the use of a lysis solution, the cells were mixed with agarose gel (LMAgarose; Trevigen) and then placed in an electrophoretic field at a constant voltage of 10 V for 10 min. Following electrophoresis, the cells were stained with the use of SYBR Green (Trevigen).

Cell-image analysis, performed with a fluorescence microscope and imaging software (TriTek CometScore, Sumerduck, VA, USA), assessed the following parameters: tail length; percentage of DNA in the tail; and tail moment. Tail length refers to the distance of damaged DNA migration from the nucleoid; percentage of DNA in the tail refers to the proportion of total DNA present in the tail; and tail moment represents the index of induced DNA damage, indicating both the migration of damaged DNA and the relative amount of DNA in the tail, derived from the percentage of DNA in the comet tail and the tail length.

Detection of Fas, Fas ligand and cytokines

Specific ELISA kits were employed for the detection of human Fas ligand (Mouse Fas ligand/TNFSF6 Immunoassay; R&D Systems) and of various cytokines, as follows: TNF-α, IL1-α, IL-β, IL-2, IL-4, IL-10, interferon-γ (IFN-γ), granulocyte-colony stimulating factor (G-CSF) and granulocyte-macrophage colony stimulating factor (GM-CSF) (Multi-Analyte ELISArray™ Kit; SABiosciences, Frederick, MD, USA). Briefly, to detect Fas ligand, the samples (controls or standards) were pipetted into microwells precoated with monoclonal antibodies specific to each substance. Following incubation, an enzyme-linked polyclonal antibody was added to the wells. In the next step, horseradish peroxidase and then the substrate solution were added to each well. The intensity of the color was measured using a microplate reader set to 450 nm, with a wavelength correction set to 540 nm (Bio-Rad Benchmark; Bio-Rad Japan).

Fas activity was detected using FAS (FL-335): sc-7886 antibody (Santa Cruz Biotechnology, Inc., Santa Cruz, CA, USA), and a previously established western blot technique was employed (26,27).

Statistical analysis

Statistical analysis was performed using unpaired *t*-test. Results from all experiments are presented as the means ± SD. Statistical significance was accepted at $p < 0.05$.

Results

Apoptosis induced by hydrogen sulfide

The number of early apoptotic cells increased as a result of H_2S incubation in a time-dependent manner compared with their respective controls (8.74 ± 3.15 vs. 2.40 ± 1.32% for 24 h; 22.44 ± 4.10 vs. 2.81 ± 1.24% for 36 h; and 21.22 ± 1.18 vs. 2.68 ± 1.18% for 48 h, $p < 0.01$ respectively, $n = 5$; Fig. 1A). Late apoptotic and necrotic cells were significantly increased for 36 and 48 h (5.87 ± 2.37 vs. 1.14 ± 0.03% for 24 h; 44.97 ± 10.47 vs. 1.71 ± 0.64% for 36 h; and 50.61 ± 9.54 vs. 1.98 ± 0.63% for 48 h, $p < 0.01$ respectively, $n = 5$; Fig. 1B). Moreover, Cell Death ELISA® assay showed that the enrichment factor, indicating the portion of detected

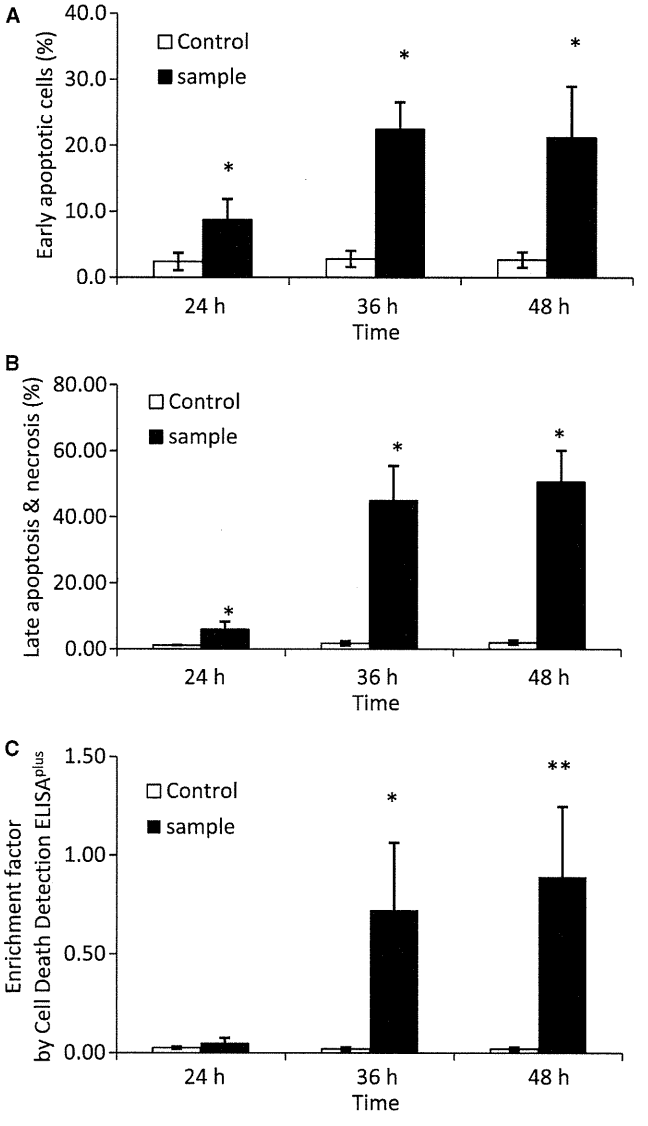

Fig. 1. Detection of early apoptosis, late apoptosis and necrosis. (A) Early apoptotic cells (%) were increased after 24, 36 and 48 h in a time-dependent manner. Each bar represents the mean ± SD of five independent experiments (*$p < 0.01$). (B) Late apoptotic and necrotic cells were also increased, especially after 36 and 48 h. Each bar represents the mean ± SD of five independent experiments (*$p < 0.01$). (C) Cell Death ELISA assay also indicated that the apoptotic cells, shown as enrichment factor, were significantly increased in a time-dependent manner. Each bar represents the mean ± SD of five independent experiments (**$p < 0.05$).

nucleosome in the cytosol of apoptotic cells, increased dramatically compared with controls for 36 and 48 h (0.72 ± 0.34 vs. 0.02 ± 0.01 for 36 h, $p < 0.01$; and 0.89 ± 0.36 vs. 0.02 ± 0.01 for 48 h, $p < 0.05$, $n = 5$; Fig. 1C).

Mitochondrial changes

Membrane depolarization of mitochondria increased at each time point following H_2S incubation (13.86 ± 1.71 vs. 3.69 ± 1.85% for 24 h; 48.07 ± 5.92 vs. 2.04 ± 1.53% for 36 h; and 49.12 ± 5.58 vs. 7.17 ± 2.52% for 48 h, $p < 0.01$ respectively, $n = 5$; Fig. 2A). Cytochrome *c* release into cytosol also increased dramatically compared with controls (1.92 ± 0.50 vs. 0.08 ± 0.01 ng/mL for 24 h, $p < 0.05$; 4.73 ± 0.96 vs. 0.12 ± 0.04 ng/mL for 36 h; and 1.17 ± 0.16 vs. 0.20 ± 0.10 ng/mL for 48 h, $p < 0.01$ for both, $n = 5$; Fig. 2B).

Caspase activities

Caspase-3, -8 and -9 were also strongly activated in H_2S-treated samples compared with their respective controls. Caspase-3, an executioner enzyme of the apoptosis process, was found to be activated significantly more than the control at each time point [8.28 ± 3.03 vs. 1.80 ± 0.65 relative fluorescence units (RFU) for 24 h, $p < 0.05$; 18.54 ± 4.97 vs. 0.41 ± 0.11 RFU for 36 h, $p < 0.01$; and 13.52 ± 4.48 vs. 3.66 ± 1.19 RFU for 48 h, $p < 0.05$, $n = 5$; Fig. 3A]. Caspase-9 activity was significantly higher in the samples than in the control (7.51 ± 3.97 vs. 1.54 ± 0.31 RFU for 24 h, $p < 0.05$; 14.64 ± 3.16 vs. 0.54 ± 0.26 RFU for 36 h; and 14.16 ± 3.61 vs. 1.15 ± 0.73 RFU for 48 h, $p < 0.01$ for both, $n = 5$; Fig. 3B). Caspase-8 activity was also increased in a time-dependent manner, with a significant difference found for 36 and 48 h (1.92 ± 0.63 vs. 1.15 ± 0.44 RFU for 24 h; 6.23 ± 0.82 vs. 0.54 ± 0.13 RFU for 36 h, and 5.19 ± 0.51 vs. 0.65 ± 0.33 RFU for 48 h, $p < 0.01$ for both 36 h and 48 h, $n = 5$; Fig. 3C).

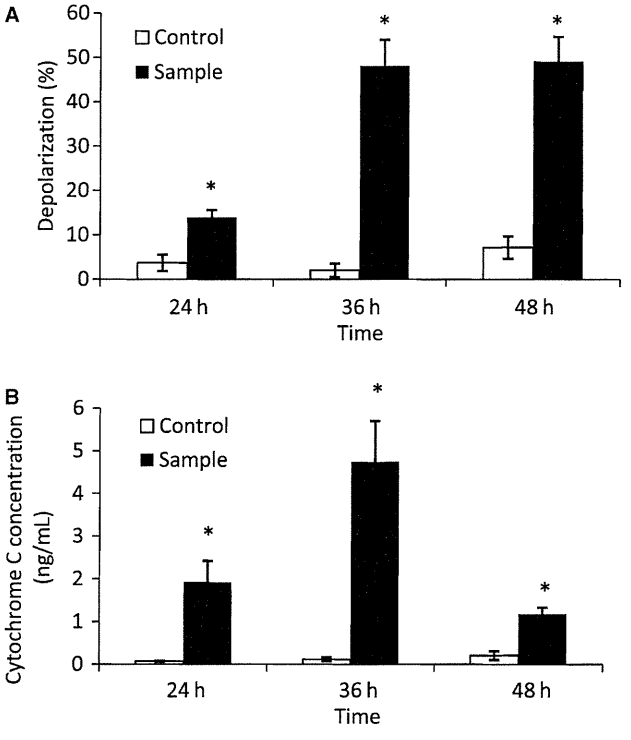

Fig. 2. Mitochondrial changes. (A) Mitochondrial membrane electrical gradient was disrupted after H_2S treatment; the percentage of cells with depolarization increased. Each bar represents the mean ± SD of five independent experiments (*$p < 0.01$). (B) Cytochrome *c* release into cytosol was also significantly increased, especially after 36 h. Each data point represents the mean ± SD of five independent experiments (*$p < 0.01$).

p53 expression

The expression of tumor-suppressor protein p53 also increased significantly compared with the controls (48.45 ± 4.76 vs. 15.04 ± 1.44 pg/mL for 24 h; 70.99 ± 5.70 vs. 12.57 ± 2.62 pg/mL for 36 h; and 72.50 ± 6.65 vs. 15.51 ± 3.82 pg/mL for 48 h, $p < 0.01$ respectively, $n = 5$; Fig. 4).

BAX and *Bcl-2* gene expression

BAX gene expression became significantly upregulated compared with controls for 36 and 48 h (7.86 ± 0.14 vs. 3.65 ± 0.47 for 36 h; and 4.51 ± 0.04 vs. 3.63 ± 0.06 for 48 h, $p < 0.01$, $n = 5$; Fig. 5A). The anti-apoptotic gene *Bcl-2* remained low following H_2S incubation; no significant difference was found compared with controls (0.57 ± 0.16 vs. 1.02 ± 0.02 for 24 h; 0.79 ± 0.13 vs. 1.31 ± 0.16 for 36 h; and 0.79 ± 0.08 vs. 1.10 ± 0.36 for 48 h, $n = 5$; Fig. 5B).

DNA fragmentation

Tail length, percentage of DNA in tail, and their product, tail moment, are all parameters that increased, indicating significantly more DNA strand breaks in test samples than in corresponding controls (Table 1).

Death ligand pathway

After both 24 and 48 h of H_2S treatment, Fas ligand, Fas receptor, TNF-α, IL1-α, IL-β, IL-2, IL-4, IL-10, IFN-γ, G-CSF and GM-CSF levels remained low, comparable to their respective control groups (data not shown).

Discussion

It has been previously established that the apoptotic process is actively involved in the initiation and development of periodontal diseases (21–23,32). One of the distinguishing characteristics of periodontitis is bone loss. The rate of bone formation and resorption is largely determined by the numbers of osteoblasts and osteoclasts present (24,25). Apoptosis could have a

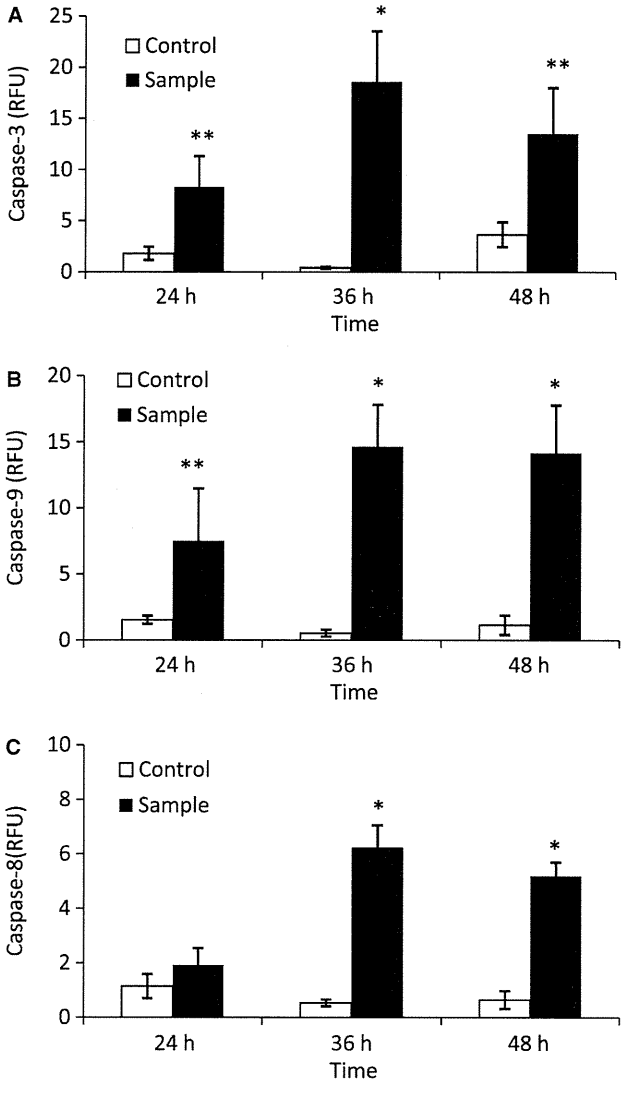

Fig. 3. Detection of caspase-3, -8 and -9 activities. (A) Caspase-3, an executioner caspase, was activated in a time-dependent manner. Each bar represents the mean ± SD of five independent experiments (*$p < 0.01$, **$p < 0.05$). (B) The activity of caspase-9, an initiator caspase, also increased in a time-dependent manner, suggesting that H_2S-induced apoptosis is activated via an intrinsic apoptotic pathway. Each bar represents the mean ± SD of five independent experiments (*$p < 0.01$, **$p < 0.05$). (C) Caspase-8 activity also increased in a time-dependent manner. Each bar represents the mean ± SD of five independent experiments (*$p < 0.01$).

significant impact on the number of osteoblasts presenting at the site of bone formation. Many reports have suggested that VSCs may accelerate the progression of periodontal disease (20–23,26,27). However, there is limited scientific evidence to explain the relationship between bone resorption and H_2S in periodontitis, although it has been proved that H_2S penetrates into alveolar bone through gingival tissues (17,20). We used 50 ng/mL of H_2S to simulate its concentration in the tissue in this study, which would approximate the lowest concentration of H_2S present in a gingival crevice or periodontal pocket (31).

In this study, we demonstrate that H_2S, at lower-than-pathological concentrations, induces apoptosis in osteoblasts. After exposure to H_2S, the number of osteoblasts at an early stage of apoptosis was significantly increased. Moreover, late apoptotic and necrotic cells also increased after H_2S treatment, but flow cytometry cannot distinguish between these two forms of cell death. Therefore, another assay, Cell Death ELISA®, was employed in this study. A significant increase in the number of apoptotic cells was found in samples exposed to H_2S compared with those not exposed to H_2S after necrotic cells were removed. Both flow cytometry and ELISA showed that H_2S caused apoptosis in osteoblasts.

DNA fragmentation was observed using single-cell gel electrophoresis. The parameters of tail length, percentage of DNA in the tail and tail moment were significantly increased. There is well-documented evidence that the tumor-suppressor protein p53 regulates the cellular response to DNA damage (32). In this study, the total p53 level was significantly increased in H_2S-exposed cells compared with their respective controls. p53 triggers one of the major pathways involved in apoptosis, the cell death ligand/receptor pathway, including caspase-8, and the intrinsic mitochondrial pathway (36).

In the intrinsic pathway, BAX, which is a pro-apoptotic member of the Bcl-2 family, is a p53-primary-response molecule (38). BAX activation mediates mitochondrial membrane depolarization, which can lead to the activation of the mitochondrial apoptotic pathway. Our RT-PCR data demonstrated that the *BAX* gene was upregulated in a time-dependent manner, but *Bcl-2*, an anti-apoptotic gene, remained low. In fact, following H_2S incubation, depolarization of the mitochondrial membrane was significantly increased.

Following membrane depolarization, cytochrome *c* is released from the mitochondrial inner membrane into the cytoplasm (39). In our study, the cytochrome *c* level in the cytoplasm of H_2S-treated cells was significantly higher than in the controls. The release of cytochrome *c* in turn initiates the apoptotic caspase cascade through activation of the initiator, caspase-9. Downstream of the apoptotic cascade is the activation of caspase-3 (40). In the present study, a significant increase in the activity of both caspase-9 and caspase-3 was found after H_2S exposure. We concluded that the intrinsic

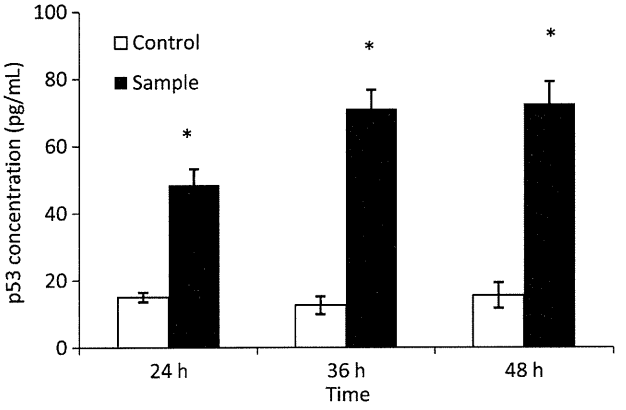

Fig. 4. Effect of H_2S on p53 levels. The expression of tumor-suppressor protein p53 increased in a time-dependent manner. Each data point represents the mean ± SD of five independent experiments (*$p < 0.01$).

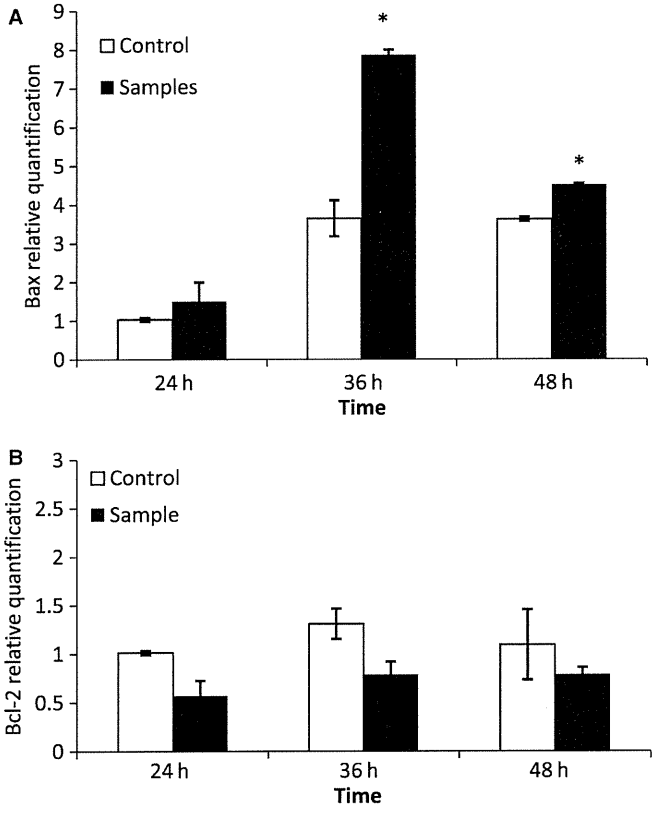

Fig. 5. Real-time quantitative RT-PCR. (A) *BAX* gene activity was upregulated, especially after 36 h. Each bar represents the mean ± SD of five independent experiments (*$p < 0.01$). (B) *Bcl-2* gene activity remained low following H_2S treatment.

mitochondrial pathway was activated by H_2S during the process of apoptosis in osteoblasts.

Both caspase-9 and caspase-8 are defined as initiator caspases that can in turn activate caspase-3 as the executor caspase of apoptosis. The extrinsic pathway, involving a receptor ligand-mediated mechanism, was also examined in this study. Caspase-8 was activated in a time-dependent manner following H_2S incubation. Caspase-8, which is activated by both inducible dimerization and inducible cleavage, is

Table 1. Genomic DNA damage

	24 h			36 h			18 h		
Group	Tail length (pixels)	DNA (%) in tail	Tail moment	Tail length (pixels)	DNA (%) in tail	Tail moment	Tail length (pixels)	DNA (%) in tail	Tail moment
Control	2.36 ± 2.28	3.99 ± 3.84	0.33 ± 0.33	3.41 ± 3.33	4.90 ± 4.83	0.29 ± 0.29	2.95 ± 2.78	4.76 ± 4.63	0.07 ± 0.07
Sample	5.85 ± 4.98*	14.16 ± 7.71*	1.37 ± 1.34*	62.62 ± 43.24*	34.06 ± 17.99*	25.35 ± 23.96*	48.22 ± 38.05*	35.01 ± 16.33*	5.88 ± 5.82*

Tail length is an expression of the distance of DNA damage migration from the nucleoid. DNA (%) in tail is an expression of the proportion of total DNA in tail. Tail moment is the product of the first two parameters, representing the extent of DNA damage. Each data point represents the mean ± SD of five independent experiments; 75 nuclei analysed per experiment (*$p < 0.01$).

a key initiator caspase in apoptosis associated with Fas, ligand-activated tumour-necrosis factor receptor-1 or tumour-necrosis factor-related apoptosis-inducing ligands (TRAILs) (34–36,41). Effector cells for TRAILs are T cells or natural killer cells (42,43). However, it is well established that TRAILs cause neither caspase-8 activation nor apoptosis in osteoblasts (44,45); moreover, no T cells or natural killer cells were found in our osteoblast culture. Therefore, caspase-8 activation in this study could not have been caused by TRAILs. Next, we measured Fas and Fas ligand activity. Both levels remained low, suggesting that they are not involved in H_2S-induced apoptosis. Several studies have shown that many cytokines, especially TNF-α, can activate caspase-8 and can initiate apoptosis in osteoblasts (46–55). Thus, we measured the activity of TNF-α, IL1-α, IL-β, IL-2, IL-4, IL-10, IFN-γ, G-CSF and GM-CSF after H_2S exposure. However, there was no difference in these cytokine levels between the test samples and their respective controls.

It has been suggested that none of the cell-death ligand receptors in the extrinsic pathway is involved, while caspase-8 is activated in the apoptotic process. In fact, many previous studies have shown that p53 directly activates the caspase-8 pathway independent of the extrinsic pathways (33–36,56–58). In this study, p53 and caspase-8 were both significantly activated at each time point after H_2S exposure, while no cell-death ligand receptors were activated. This result suggests that caspase-8 activation by H_2S might be directly associated with p53, as described by others (33–36,56–58).

In conclusion, our study determined that H_2S, at concentrations normally found in human gingival crevicular fluid, induces apoptosis in osteoblasts. The molecular mechanisms underlying the apoptotic process include p53, a mitochondrial pathway and caspase-8 activation.

Acknowledgements

This research was supported by Grant-In-Aid No. 20390538 from the Japanese Ministry of Education, Culture, Sports, Science and Technology, Tokyo, Japan. The osteoblastic cell line MC3T3-E1, derived from newborn mouse calvaria, was a kind gift from Dr H. Sudo of Ohu University, Koriyama, Japan.

References

1. Van den Velde S, van Steenberghe D, Van Hee P, Quirynen M. Detection of odorous compounds in breath. *J Dent Res* 2009;**88:**285–289.
2. Yaegaki K, Sanada K. Volatile sulfur compounds in mouth air from clinically healthy subjects and patients with periodontal disease. *J Periodontal Res* 1992;**27:**233–238.
3. Tanaka M, Yamamoto Y, Kuboniwa M *et al.* Contribution of periodontal pathogens on tongue dorsa analyzed with real-time PCR to oral malodor. *Microbes Infect* 2004;**6:**1078–1083.
4. Kurata H, Awano S, Yoshida A, Ansai T, Takehara T. The prevalence of periodontopathogenic bacteria in saliva is linked to periodontal health status and oral malodour. *J Med Microbiol* 2008;**57:**636–642.
5. Tanaka M, Anguri H, Nonaka A *et al.* Clinical assessment of oral malodor by the electronic nose system. *J Dent Res* 2004;**83:**317–321.
6. Kostelc JG, Zelson PR, Preti G, Tonzetich J. Quantitative differences in volatiles from healthy mouths and mouths with periodontitis. *Clin Chem* 1981;**27:**842–845.
7. Coli JM, Tonzetich J. Characterization of volatile sulphur compounds production at individual gingival crevicular sites in humans. *J Clin Dent* 1992;**3:**97–103.
8. Ratcliff PA, Johnson PW. The relationship between oral malodor, gingivitis, and periodontitis. A review. *J Periodontol* 1999;**70:**485–489.
9. Tsai CC, Chou HH, Wu TL *et al.* The levels of volatile sulfur compounds in mouth air from patients with chronic periodontitis. *J Periodontal Res* 2008;**43:**186–193.
10. Horowitz A, Folke LE. Hydrogen sulfide production in the periodontal environment. *J Periodontol* 1973;**44:**390–395.
11. Morita M, Wang HL. Association between oral malodor and adult periodontitis: a review. *J Clin Periodontol* 2001;**28:**813–819.
12. John M, Vandana KL. Detection and measurement of oral malodour in periodontitis patients. *Indian J Dent Res* 2006;**17:**2–6.
13. Bosy A, Kulkarni GV, Rosenberg M, McCulloch CA. Relationship of oral malodor to periodontitis: evidence of independence in discrete subpopulations. *J Periodontol* 1994;**65:**37–46.
14. Yaegaki K. Oral malodorous compounds are periodontally pathogenic and carcinogenic. *Jpn Dent Sci Rev* 2008;**44:**100–108.
15. Eghbal MA, Pennefather PS, O'Brien PJ. H_2S cytotoxicity mechanism involves reactive oxygen species formation and mitochondrial depolarisation. *Toxicology* 2004;**203:**69–76.
16. Rizzo AA. The possible role of hydrogen sulfide in human periodontal disease. I. Hydrogen sulfide production in periodontal pockets. *Periodontics* 1967;**5:**233–236.
17. Irie K, Ekuni D, Yamamoto T *et al.* A single application of hydrogen sulphide induces a transient osteoclast differentiation with RANKL expression in the rat model. *Arch Oral Biol* 2009;**54:**723–729.
18. Johnson P, Yaegaki K, Tonzetich J. Effect of methyl mercaptan on synthesis and degradation of collagen. *J Periodontal Res* 1996;**31:**323–329.
19. Johnson PW, Yaegaki K, Tonzetich J. Effect of volatile thiol compounds on protein metabolism by human gingival fibroblasts. *J Periodontal Res* 1992;**27:**553–561.
20. Ng W, Tonzetich J. Effect of hydrogen sulfide and methyl mercaptan on the permeability of oral mucosa. *J Dent Res* 1984;**63:**994–997.
21. Yaegaki K, Qian W, Murata T *et al.* Oral malodorous compound causes apoptosis and genomic DNA damage in human gingival fibroblasts. *J Periodontal Res* 2008;**43:**391–399.
22. Calenic B, Yaegaki K, Murata T *et al.* Oral malodorous compound triggers mitochondrial-dependent apoptosis and causes genomic DNA damage in human gingival epithelial cells. *J Periodontal Res* 2010;**45:**31–37.
23. Fujimura M, Calenic B, Yaegaki K *et al.* Oral malodorous compound activates mitochondrial pathway inducing apoptosis in human gingival fibroblasts. *Clin Oral Investig* 2010;**14:**367–373.
24. Jilka RL, Weinstein RS, Bellido T, Parfitt AM, Manolagas SC. Osteoblast programmed cell death (apoptosis): modulation by growth factors and cytokines. *J Bone Miner Res* 1998;**13:**793–802.
25. Yamamoto S, Mogi M, Kinpara K, *et al.* Anti-proliferative capsular-like polysaccharide antigen from *Actinobacillus actinomycetemcomitans* induces apoptotic cell death in mouse osteoblastic MC3T3-E1 cells. *J Dent Res* 1999;**78:**1230–1237.
26. Imai T, Ii H, Yaegaki K, Murata T, Sato T, Kamoda T. Oral malodorous compound inhibits osteoblast proliferation. *J Periodontol* 2009;**80:**2028–2034.
27. Ii H, Imai T, Yaegaki K, Irie K, Ekuni D, Morita M. Oral malodorous compound induces osteoclast differentiation without

receptor activator of nuclear factor κB ligand. *J Periodontol* 2010;**81:**1691–1697.
28. Yu YP, Li ZG, Wang DZ, Zhan X, Shao JH. Hydrogen sulfide as an effective and specific novel therapy for acute carbon monoxide poisoning. *Biochem Biophys Res Commun* 2011;**404:**6–9.
29. Lavu M, Bhushan S, Lefer D. Hydrogen sulfide-mediated cardioprotection: mechanisms and therapeutic potential. *Clin Sci (Lond)* 2010;**120:**219–229.
30. Shi S, Li QS, Li H *et al.* Anti-apoptotic action of hydrogen sulfide is associated with early JNK inhibition. *Cell Biol Int* 2009;**33:**1095–1101.
31. Persson S. Hydrogen sulfide and methyl mercaptan in periodontal pockets. *Oral Microbiol Immunol* 1992;**7:**378–379.
32. Calenic B, Yaegaki K, Kozhuharova A, Imai T. Oral malodorous compound causes oxidative stress and p53-mediated programmed cell death in keratinocyte stem cells. *J Periodontol* 2010;**81:**1317–1323.
33. Hama-Inaba H, Choi KH, Wang B *et al.* Fas-independent apoptosis induced by UVC in p53-mutated human epithelial tumor A431 cells through activation of caspase-8 and JNK/SAPK. *J Radiat Res (Tokyo)* 2001;**42:**201–215.
34. Ding HF, McGill G, Rowan S, Schmaltz C, Shimamura A, Fisher DE. Oncogene-dependent regulation of caspase activation by p53 protein in a cell-free system. *J Biol Chem* 1998;**273:**28378–28383.
35. Ding HF, Lin YL, McGill G *et al.* Essential role for caspase-8 in transcription-independent apoptosis triggered by p53. *J Biol Chem* 2000;**275:**38905–38911.
36. Haupt S, Berger M, Goldberg Z, Haupt Y. Apoptosis – the p53 network. *J Cell Sci* 2003;**116:**4077–4085.
37. Livak KJ, Schmittgen TD. Analysis of relative gene expression data using real-time quantitative PCR and the $2^{-\Delta\Delta C}{}_T$ method. *Methods* 2001;**25:**402–408.
38. Chipuk JE, Kuwana T, Bouchier-Hayes L *et al.* Direct activation of Bax by p53 mediates mitochondrial membrane permeabilization and apoptosis. *Science* 2004;**303:**1010–1014.
39. Hearps AC, Burrows J, Connor CE *et al.* Mitochondrial cytochrome *c* release precedes transmembrane depolarisation and caspase-3 activation during ceramide-induced apoptosis of Jurkat T cells. *Apoptosis* 2002;**7:**387–394.
40. Saunders PA, Cooper JA, Roodell MM *et al.* Quantification of active caspase 3 in apoptotic cells. *Anal Biochem* 2000;**284:**114–124.
41. Oberst A, Pop C, Tremblay AG *et al.* Inducible dimerization and inducible cleavage reveal a requirement for both processes in caspase-8 activation. *J Biol Chem* 2010;**285:**16632–16642.
42. Rus V, Nguyen V, Puliaev R *et al.* T cell TRAIL promotes murine lupus by sustaining effector CD4 Th cell numbers and by inhibiting CD8 CTL activity. *J Immunol* 2007;**178:**3962–3972.
43. Hayakawa Y, Screpanti V, Yagita H *et al.* NK cell TRAIL eliminates immature dendritic cells in vivo and limits dendritic cell vaccination efficacy. *J Immunol* 2004;**172:**123–129.
44. Atkins GJ, Bouralexis S, Evdokiou A *et al.* Human osteoblasts are resistant to Apo2L/TRAIL-mediated apoptosis. *Bone* 2002;**31:**448–456.
45. Bu R, Borysenko CW, Li Y *et al.* Expression and function of TNF-family proteins and receptors in human osteoblasts. *Bone* 2003;**33:**760–770.
46. Son YO, Kook SH, Choi KC *et al.* Quercetin, a bioflavonoid, accelerates TNF-alpha-induced growth inhibition and apoptosis in MC3T3-E1 osteoblastic cells. *Eur J Pharmacol* 2006;**529:**24–32.
47. Chua CC, Chua BH, Chen Z *et al.* TGF-beta1 inhibits multiple caspases induced by TNF-alpha in murine osteoblastic MC3T3-E1 cells. *Biochim Biophys Acta* 2002;**1593:**1–8.
48. Suh KS, Koh G, Park CY *et al.* Soybean isoflavones inhibit tumor necrosis factor-alpha-induced apoptosis and the production of interleukin-6 and prostaglandin E2 in osteoblastic cells. *Phytochemistry* 2003;**63:**209–215.
49. Kim KB, Choi YH, Kim IK *et al.* Potentiation of Fas- and TRAIL-mediated apoptosis by IFN-gamma in A549 lung epithelial cells: enhancement of caspase-8 expression through IFN-response element. *Cytokine* 2002;**20:**283–288.
50. Hopkins-Donaldson S, Ziegler A, Kurtz S *et al.* Silencing of death receptor and caspase-8 expression in small cell lung carcinoma cell lines and tumors by DNA methylation. *Cell Death Differ* 2003;**10:**356–364.
51. Shankaranarayanan P, Nigam S. IL-4 induces apoptosis in A549 lung adenocarcinoma cells: evidence for the pivotal role of 15-hydroxyeicosatetraenoic acid binding to activated peroxisome proliferator-activated receptor gamma transcription factor. *J Immunol* 2003;**170:**887–894.
52. Adachi Y, Taketani S, Ikehara S *et al.* Apoptosis of colorectal adenocarcinoma induced by 5-FU and/or IFN-gamma through caspase 3 and caspase 8. *Int J Oncol* 1999;**15:**1191–1196.
53. Refaeli Y, Van Parijs L, London CA, Tschopp J, Abbas AK. Biochemical mechanisms of IL-2-regulated Fas-mediated T cell apoptosis. *Immunity* 1998;**8:**615–623.
54. Thorburn J, Frankel AE, Thorburn A. Apoptosis by leukemia cell-targeted diphtheria toxin occurs via receptor-independent activation of Fas-associated death domain protein. *Clin Cancer Res* 2003;**9:**861–865.
55. Schmidt-Mende J, Tehranchi R, Forsblom AM, Joseph B, Hellström-Lindberg E *et al.* Granulocyte colony-stimulating factor inhibits Fas-triggered apoptosis in bone marrow cells isolated from patients with refractory anemia with ringed sideroblasts. *Leukemia* 2001;**15:**742–751.
56. Liu JJ, Nilsson A, Oredsson S *et al.* Boswellic acids trigger apoptosis via a pathway dependent on caspase-8 activation but independent on Fas/Fas ligand interaction in colon cancer HT-29 cells. *Carcinogenesis* 2002;**23:**2087–2093.
57. Jones DT, Ganeshaguru K, Virchis AE *et al.* Caspase 8 activation independent of Fas (CD95/APO-1) signaling may mediate killing of B-chronic lymphocytic leukemia cells by cytotoxic drugs or gamma radiation. *Blood* 2001;**98:**2800–2807.
58. Schuler M, Green DR. Mechanisms of p53-dependent apoptosis. *Biochem Soc Trans* 2001;**29:**684–688.

Standardization of clinical protocols in oral malodor research

2012 J. Breath Res. 6 017101

(http://iopscience.iop.org/1752-7163/6/1/017101)

IOP PUBLISHING JOURNAL OF BREATH RESEARCH

J. Breath Res. 6 (2012) 017101 (10pp) doi:10.1088/1752-7155/6/1/017101

Standardization of clinical protocols in oral malodor research

Ken Yaegaki[1,2,5], Donald M Brunette[2], Albert Tangerman[3], Yong-Sahm Choe[4], Edwin G Winkel[3], Sayaka Ito[1], Tomohiro Kitano[1], Hisataka Ii[1], Bogdan Calenic[1], Nikolay Ishkitiev[1] and Toshio Imai[1]

[1] Department of Oral Health, Nippon Dental University, 1-9-20 Fujimi, Chiyodaku, Tokyo, Japan
[2] Department of Oral Biological and Medical Sciences, University of British Columbia Faculty of Dentistry, 2199 Wesbrook Mall, Vancouver, BC, Canada
[3] Academic Center for Oral Health, Department of Periodontology, University Medical Center Groningen, A. Deusinglaan 1, 9713 AV Groningen, The Netherlands
[4] iSenLab, 186 Galmachi-ro, Sangdaewon-dong, Jungwon-gu, Seongnam-si, Gyeonggi-do, Korea

E-mail: yaegaki-k@tky.ndu.ac.jp

Received 1 September 2011
Accepted for publication 30 January 2012
Published 27 February 2012
Online at stacks.iop.org/JBR/6/017101

Abstract

The objective of this study is to standardize protocols for clinical research into oral malodor caused by volatile sulfur compounds (VSCs). To detect VSCs, a gas chromatograph (GC) using a flame photometric detector equipped with a bandpass filter (at 393 nm) is the gold standard (sensitivity: 5×10^{-11} gS s^{-1}). The baselines of VSC concentrations in mouth air varied considerably over a week. When the subjects refrained from eating, drinking and oral hygiene including mouth rinsing, the VSC concentrations remained constant until eating. Over a 6 h period after a meal, VSC concentrations decreased dramatically ($p < 0.01$). These results point to optimal times and conditions for sampling subjects. Several portable devices were compared with the measurements by the GCs. Portable GCs demonstrated capabilities similar to those of the GCs. We also applied the recommended protocols described below to clinical research testing the efficacy of $ZnCl_2$ products, and confirmed that using the recommended protocols in a randomized crossover design would provide very clear results. Proposed protocols include: (a) a short-term study rather than a long-term study is strongly recommended, since the VSC concentrations are constant in the short term; (b) a crossover study would be the best design to avoid the effects of individual specificities on each clinical intervention; (c) measurements of VSCs should preferably be carried out using either a GC or portable GCs.

(Some figures may appear in colour only in the online journal)

Introduction

Halitosis is caused by oral, systemic, or psychological conditions and may be classified accordingly as *genuine halitosis*, *pseudo-halitosis* or *halitophobia* [1–3]. *Genuine halitosis* is subclassified as either *physiological* or *pathological*, and the latter can be either *intraoral* or *extraoral* in origin.

In this paper, the focus is on oral malodor, i.e. physiological and intraoral pathological halitosis. Measuring oral malodor strength is an important step in the process of diagnosing halitosis. In the clinic, organoleptic measurement is the most popular diagnostic procedure [1, 2, 4, 5]. Given that there are nearly 700 different compounds found in mouth air [6], it is difficult to determine objectively their concentrations in a clinical setting by any method. [7–11]. However, studies have shown that only volatile sulfur compounds (VSCs) composed of hydrogen sulfide (H_2S), methyl mercaptan (CH_3SH), and dimethyl sulfide ($[CH_3]_2S$) correlate with oral malodor strength [6, 12]. Other compounds, including cadaverine, are insignificant in producing oral malodor [6].

[5] Author to whom any correspondence should be addressed.

Weber's law of perceptual psychology states that a logarithmic relation is found between the physical magnitude of stimuli (in this instance log VSC concentration) and the perceived intensity of the stimuli (odor strength). This law has been found to apply in the correlation between VSCs in mouth air and oral malodor strength [4]. Consequently, objectively measuring VSCs is a much more reliable method of judging its strength than simple organoleptic measurement. A gas chromatography (GC) test to measure VSCs is the most effective method to diagnose halitosis and should be considered the 'gold standard' [1–3, 5, 12–15]. However, most breath clinics make use of portable sulfide monitors such as the Halimeter™ (Interscan, Chatsworth, CA) [16, 17], which may detect other compounds in mouth air [18–20], or the Breathtron™ (New Cosmos Electric, Osaka, Japan) [21, 22] to measure VSCs. These devices cannot distinguish the components of VSCs [16, 17, 23–28] and are very sensitive to other organic compounds as well [5, 16, 19, 25–29]. Two portable GCs, the OralChroma™ (Abilit, Osaka, Japan) and the Twin Breasor (GC, Tokyo, Japan), have been developed to detect VSCs. In this paper, we determine the accuracy of these portable detectors to establish the recommended protocols of oral malodor research.

The protocols of oral malodor clinical research are divided generally into two categories, i.e. short-term and long-term protocols. The correct protocol for measuring VSCs is not yet well understood [28]. Several protocols for performing long-term clinical studies to measure the baselines of VSCs or malodor have been developed [11, 30–35]. The premise of the research design on which they are based is that the baseline must be constant for several days or weeks during the experiments. Moreover, although some research designs include meals during the testing time or allow the subjects to eat before measurements [11, 30–35], the effects of eating on VSC concentrations in mouth air are still obscure [1–3, 5, 36]. The aim of this study is to establish practical and standardized protocols employing VSC measurement for clinical studies of halitosis.

Materials and methods

Studies on the effects of meals on VSC concentrations in mouth air during a day and on the changes of VSC concentration over a week were carried out using a conventional GC. The results of mouth-air analyses by portable VSC detectors were compared with the results from a conventional GC. Since baseline concentrations of VSCs in mouth air fluctuate over a week but are constant for several hours, as described later, novel research protocols for short-term clinical studies were applied to a clinical study of $ZnCl_2$ oral-hygiene products intended to reduce oral malodor, and a conventional GC was employed to detect VSCs in mouth air. Moreover, a randomized crossover study was designed to avoid the effects of individual specificities on each clinical intervention.

Subject selection

All subjects affirmed that they were not suffering from any known disease including periodontitis nor receiving any medical treatment. For part of this study, cystinotic patients were employed as described later. For the baseline measurements of VSCs, the volunteers were asked to refrain from eating, drinking, and all oral hygiene practices from midnight until the end of each experiment. All subjects signed informed consent forms, and the protocol was approved by the ethics committees of the Nippon Dental University, the University of British Columbia, and Groningen University.

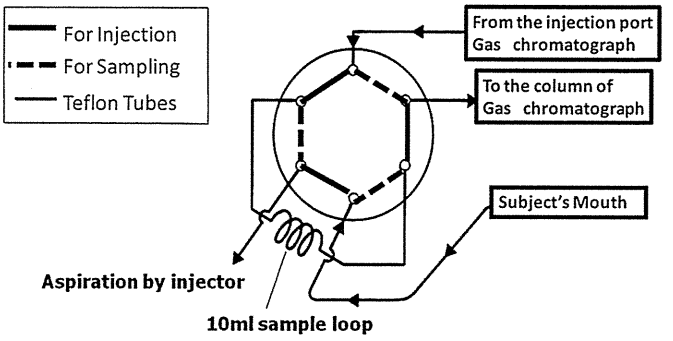

Figure 1. The GCs were modified to inject precisely 10 ml samples of gas by connection of the 6-port valve and 10 ml sample loop. This system allows us to inject an exact volume of sample air without any backpressure.

Mouth-air analysis by GC

Mouth-air samples were analyzed with the use of a conventional GC employing a flame photometric detector (sensitivity: 5×10^{-11} gS s^{-1}) equipped with a bandpass filter (at 393 nm) (GC-8APFP or GC-14APFP, Shimadzu, Kyoto, Japan). Teflon columns (3 mm inner diameter × 3 m) packed with 25% (1, 2, 3-Tris (2-cyanoethoxy) propane 80–100 mesh (Shimadzu) were installed in the GC systems. Some other studies have employed a gas-tight syringe for sampling and injecting a large volume of sample into a GC [37, 38]. However, a large backpressure of carrier gas increases the dead volume of the syringe, thus producing inaccurate measurements [5]. The GCs were, therefore, modified to inject precisely 10 ml samples of gas (i.e. a 10 ml sample loop was incorporated into the carrier gas line with a 6-port valve) (figure 1). The GC was calibrated with the standard gases of VSCs produced from Dynacal Permeationtubes™ (VICI Metronics, Poulsbo, WA, USA) in Dynacalibrator™ (VICI Metronics), or standard permeation tubes (Gastec, Kanagawa, Japan) in a Permeater™ gas generator (Gastec). VSC concentrations were expressed as ng/10 ml or ppb [3, 12, 16, 17, 22]. Sampling for both the GC and a portable VSC detector was carried out at the same time as described previously [29].

Changes in baselines of VSCs in mouth air during one week

The protocol currently recommended for obtaining baseline measurements of VSCs [11, 30–35, 39–41]. In the present study, we determined whether the baselines of VSCs in mouth air remain constant over the course of one week. Since a small change in concentration becomes a much larger change in percentage value in subjects with lower VSC concentrations than in subjects with higher VSC concentrations, we separated

the subjects into two groups: those who demonstrated less than 5 ng/10 ml mouth air and those who demonstrated more than 5 ng/10 ml mouth air [4]. The subjects were asked to refrain from eating, drinking and all oral-hygiene practices from 12:00 midnight until completing VSC measurements at 10 AM. Changes (%) in VSC baseline in mouth air were determined every third or fourth day during a one-week period, using the conventional GC system described above.

Effects of meals on VSC concentrations during a day

The subjects were asked to refrain from eating, drinking and all oral-hygiene practices from 12:00 midnight until lunch time, and were asked to follow the same restrictions after meals. These restrictions ensured a constant concentration of VSCs in the subjects' mouths throughout the morning until they have meals. VSC concentrations were determined by a conventional GC system during the day until 6 h after lunch.

Portable VSCs detectors

For the Halimeter™ measurements, we followed the manufacturer's instructions. Briefly, to 'incubate' the mouth-breath sample, subjects were instructed to close their mouths and breathe as necessary through their noses for at least 1 min. The straw was then inserted into the nearly closed mouth, the Halimeter™ extracted the gas sample from the mouth, and peak value was recorded. The average value of two measurements was obtained. The data were compared with the results obtained from GC analyses described below.

The Breathtron™, which is a semiconductor type of sulfide monitor, uses an acidic silica-gel filter to eliminate other volatile compounds such as ketones or alcohols. We followed the manufacturer's instructions [22]. The mouthpiece connected by means of a Teflon tube attached to the sample inlet was inserted into the oral cavity. The data were compared with the results obtained from conventional GC analyses described below.

The OralChroma™ is a portable GC. The GC column consists of a Teflon column (5 mm inner diameter × 300 mm length) packed with 25% oxydipropionitrile (ODPN) supported on Celite (GL Science, Tokyo, Japan). Ambient air is used for the carrier gas. VSCs are detected by a semiconductor (In_2O_3) gas sensor [26, 29]. We followed the manufacturer's instructions. The concentrations of the three VSCs were displayed in either ng/10 ml or ppb. The data were compared with the results obtained from GC analyses described below.

A modified protocol for the OralChroma™ was also examined in this study [27]. The manufacturer's instructions specify that the amount of sample injected into the OralChroma™ must be set at 0.5 ml. To make the method more sensitive, an amount of 1 ml was injected as described previously [27]. A data-handling software system (model CHM-T1; Abi Medical, Osaka, Japan) was connected to a personal computer to display the chromatogram. Peak heights expressed in mV, measured by hand from the image on the computer screen, were used as the values of the VSCs, since perfect linear correlations were found between the levels of VSC concentrations and the measured peak heights in the range 0 to 1000 ppb [27].

Recently, a novel portable GC, Twin Breasor™, was developed by GC Co. (Tokyo, Japan). After the device had warmed up for several minutes, sample air was taken using a mouthpiece (GC) and Teflon tubing, which was connected to the instrument's inlet. With the mouthpiece inserted into their closed mouths, subjects were instructed to breathe through their noses to 'incubate' the mouth-air sample for 1 min. The Twin Breasor™ extracted 10 ml of gas sample from the mouth, then the device showed VSC values in ng/10 ml. An average value was obtained from two measurements. GC measurements were carried out at the same time.

Application of proposed protocols to clinical studies

Zinc compounds are well documented to be among the best substances for controlling VSC concentrations in mouth air [39, 41]. Ten subjects (6 men and 4 women) aged 21 to 56 years (mean 32.9 ± 15.4 years) were recruited for this study, which compared the effects of several products containing 0.1% zinc chloride. Each volunteer, screened previously, met the further following criteria: (i) a minimum of 24 existing teeth, (ii) absence of fixed or removable prostheses or orthodontic appliances, (iii) no antibiotic treatment for a three-week period prior to the experiments, (iv) no regular medication with anti-inflammatory compounds, (v) no use of tobacco products, and (vi) no pregnancy or lactation. This trial was designed as a randomized four-treatment crossover study. A one-week washout period was provided between each set of two treatments. During the trial, participants were instructed to follow their regular diet and oral hygiene procedures, but regular dental visits were prohibited.

Tongue paste containing 0.1% zinc chloride (BreathBalance® tongue paste, GC), mouthwash containing 0.1% zinc chloride (BreathBalance® mouthwash, GC), and mouth spray containing 0.1% zinc chloride (BreathBalance® spray, GC) were employed in this study. To apply the paste to the tongue, a tongue brush (Zetu-fresh®, GC) was used. Briefly, 0.3 g of the paste was evenly distributed on the brush, which was then used by the subjects to brush the tongue surface very lightly from the terminal sulcus to the apex. The paste allows brushing of the tongue without abrasion. The subjects were trained to exert a brushing pressure of less than 100 g by calibrating their perceptions of force using a kitchen scale. The subjects brushed three times on each area of the tongue dorsum separately: right side, middle, and left side. For testing the mouthwash, the subjects were instructed to rinse for 30 s with 20 ml of the mouthwash. Four separate treatment protocols were tested: (1) application of the tongue paste as described above; (2) application of the tongue paste followed by rinsing with mouthwash (that is, immediately after using the tongue paste, the subjects rinsed with 20 ml of the mouthwash); (3) rinsing with 20 ml of the mouthwash alone; and (4) application of the spray (approximately 0.1 ml) to the tongue dorsum three times.

To determine the concentration of VSCs, a GC was employed as described above. On the day of each treatment,

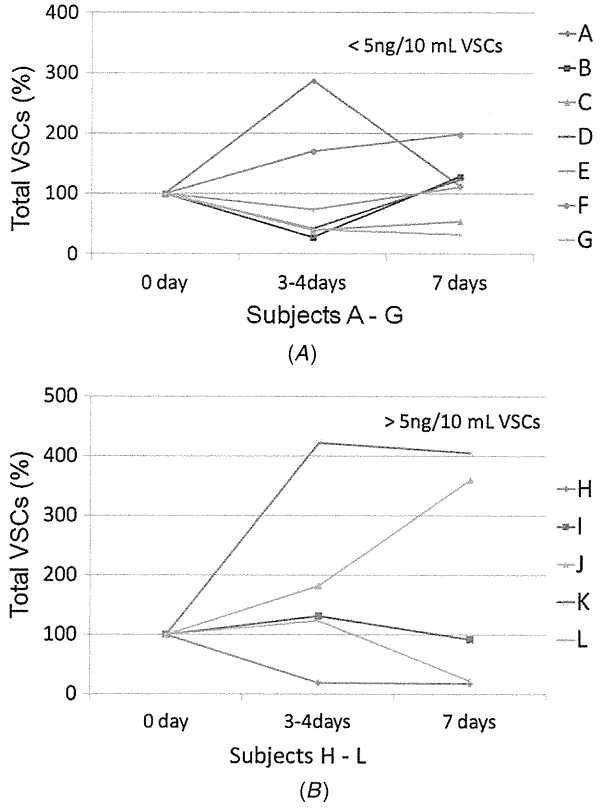

Figure 2. (*A*) Changes in VSC concentration (%) in the lower VSC concentration group during a one-week period. Huge validity of VSC concentration during a week was found, but subject E showed relatively constant values (less than 50% change) during a week. (*B*) Changes in VSC concentration (%) in the higher VSC concentration group during a one-week period. Huge validity of VSC concentration during a week was also found, but subject I showed relatively constant values during a week.

the subjects were asked to follow the same restrictions shown above in the section headed *Effects of meals on VSC concentrations* during a day. Mouth-air samples were analyzed before treatment (baseline); immediately after treatment (0 h); and at 1 h, 2 h and 3 h intervals after treatment. Each measurement was taken twice and then averaged (ng/10 ml) as previously reported [40].

Statistics

For multiple comparisons statistical analysis was performed with the Bonferroni method using Windows SPSS version 16, and Pearson correlation coefficient was also obtained. Statistical significance was accepted at a p-value of less than 0.05.

Results

Changes in baselines of VSCs in mouth air during one week

No subject demonstrated a constant VSC concentration. The subjects showed very variable VSC concentrations during the week. Only two subjects, E and I, showed relatively constant values of percentage changes of VSC during the week compared with others (figure 2).

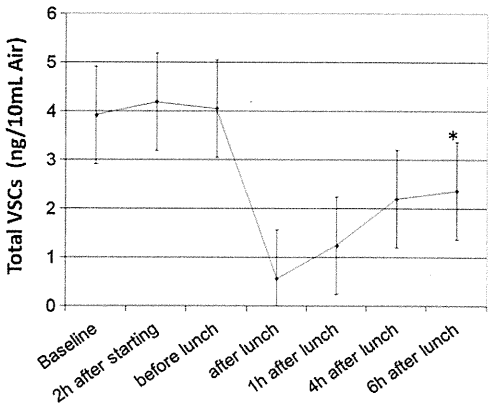

Figure 3. Effects of eating on VSC concentrations during a day. The subjects refrained from oral hygiene activities and eating until lunchtime. Prior to lunch, VSC concentrations remained constant; no significant differences were observed. However, VSC concentrations declined significantly once the subjects ate lunch (Bonferroni: $p < 0.01$, $n = 10$). After lunch, VSC concentrations continually increased for the next 6 h.

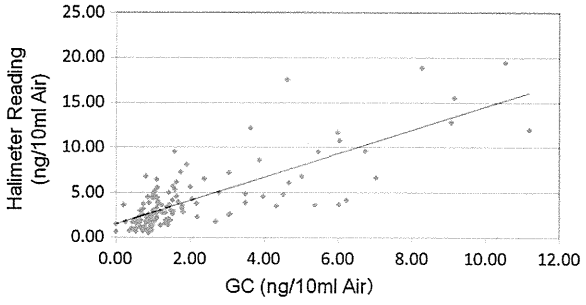

Figure 4. Halimeter^{TM} readings compared with H_2S concentrations determined by a Shimadzu GC-8APFP. Significant correlation was found ($R = 0.70$, $y = 1.30x + 1.48$, $p < 0.0001$), but the coefficient of determination was less than 0.5 ($n = 127$).

Effects of meals on VSC concentrations during a day

The protocols of many clinical investigators include meals during the intervention term and/or before the measurement of malodor before and after treatments [8, 32, 34, 35, 41]. In this study, the effects of meals on VSC concentrations during the course of one day were measured, as shown in figure 3. During the entire period leading to lunchtime VSC concentrations remained constant, and no significant difference was observed among the evaluation points prior to lunch. However, VSC concentrations declined dramatically after lunch ($p < 0.01$) and then continually increased for a period of up to 6 h. Nevertheless, VSC measurements taken at 6 h after lunch revealed that VSC concentrations were still significantly lower than at the baseline ($p < 0.01$).

Halimeter^{TM}

While significant correlation was found ($y = 1.30y + 1.48$, $p < 0.0001$), the coefficient of determination was less than 0.5 ($R = 0.70$, $n = 127$) (figure 4). A modified protocol that measures plateau values instead of peak values during Halimeter readings had been used previously, producing very high correlations (e.g., $R = 0.97$) between GC measurements

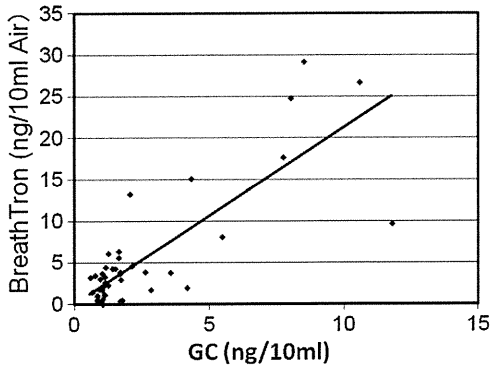

Figure 5. BreathTron™ readings compared with H_2S concentrations determined by a Shimadzu GC-8APFP. Significant correlation was found ($R = 0.89$, $y = 2.13x$, $p < 0.0001$, $n = 44$).

and Halimeter™ readings [16]. However, we found that misdiagnosis occurred frequently and we found no correlation between the two readings mentioned above (data not shown).

Breathtron™

We compared the Breathtron readings and GC-8APFP (Shimadzu) measurements, and significant correlation was found ($R = 0.89$, $y = 2.13x$, $p < 0.0001$, $n = 44$) (figure 5). However, we found misdiagnosis frequently happens. To determine the existence of halitosis, clinicians must judge if the reading of a detector is over or under the H_2S and/or CH_3SH thresholds; the detectors sometimes cannot read VSC concentration at threshold levels accurately.

OralChroma™

The OralChroma™ display readings and GC-8APFP (Shimadzu) measurements were compared, and significant correlations were found for H_2S ($R = 0.80$, $y = 2.25x$, $p < 0.0001$, $n = 253$) (figure 6(*A*)) and for CH_3SH ($R = 0.55$, $y = 1.06x$, $p < 0.0001$, $n = 253$) (figure 6(*B*)), but no correlation was found for $(CH_3)_2S$ (figure 6(*C*)). For CH_3SH measurements, we found that the coefficient of determination was 0.3; hence, measurements for both CH_3SH and $(CH_3)_2S$, especially the latter, were unreliable.

The explanation for this outcome is that the concentrations of VSCs given by the OralChroma™ are sometimes completely incorrect due to improper assignment of the place of the VSC peaks in the chromatogram, as shown in figures 6(*B*) and (*C*). In the left panel of figure 7, the assignment of H_2S, CH_3SH and $(CH_3)_2S$ (dotted lines) is correct, resulting in reliable values for the concentrations. However, in the right panel the assignment is incorrect, and shows a lower concentration of H_2S and zero concentrations of CH_3SH and $(CH_3)_2S$ on the display. We also found that contaminated room air produced poor correlations between OralChroma™ display readings and GC measurements (data not shown). Therefore, we employed the method of Tangerman and Winkel [25] to assign each VSC peak correctly. Since $(CH_3)_2S$ measurement following the manufacturer's instructions failed to show any correlation

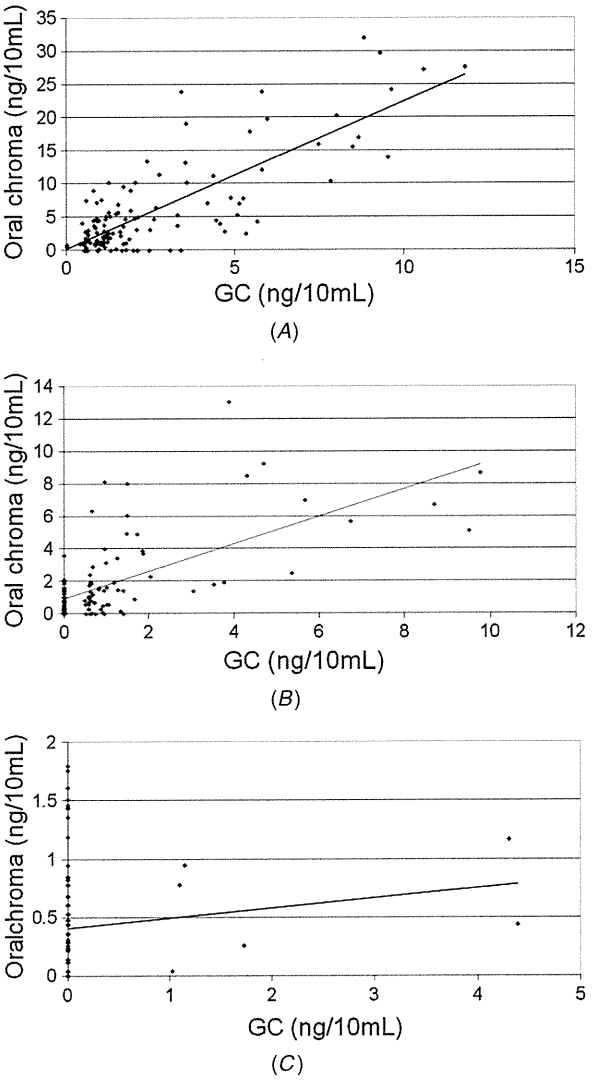

Figure 6. (*A*) The correlation between OralChroma™ display readings and GC measurements for H_2S in mouth air. A significant correlation was found ($R = 0.80$, $y = 2.25x$, $p < 0.0001$, $n = 253$). (*B*) The correlation between OralChroma™ display readings and GC measurements for CH_3SH in mouth air. A significant correlation was found ($R = 0.55$, $y = 1.06x$, $p < 0.0001$, $n = 253$). (*C*) The correlation between OralChroma™ display readings and GC measurements for $(CH_3)_2S$ in mouth air. No correlation was found.

between OralChroma™ readings and GC measurements (figure 6(*C*)), the OralChroma™ concentrations obtained by the modified protocol were compared with those obtained by a GC. Under those conditions, the correlations were almost perfect (figure 8). The data for figure 8 were obtained from a study in cystinotic patients receiving cysteamine, a drug that gives rise to elevations of $(CH_3)_2S$ concentrations. We also found that the detection limit of the OralChroma™ employing the modified protocol was 0.54 ng/10 ml for each VSC [25].

Novel portable GC: Twin Breasor™

By comparing the Twin Breasor™ display readings and GC-8APFP (Shimadzu) measurements, almost complete correlations were found for H_2S ($R = 0.97$, $y = 1.07x - 0.04$, $p < 0.0001$, $n = 137$) (figure 9(*A*)), and for CH_3SH ($R = 0.90$,

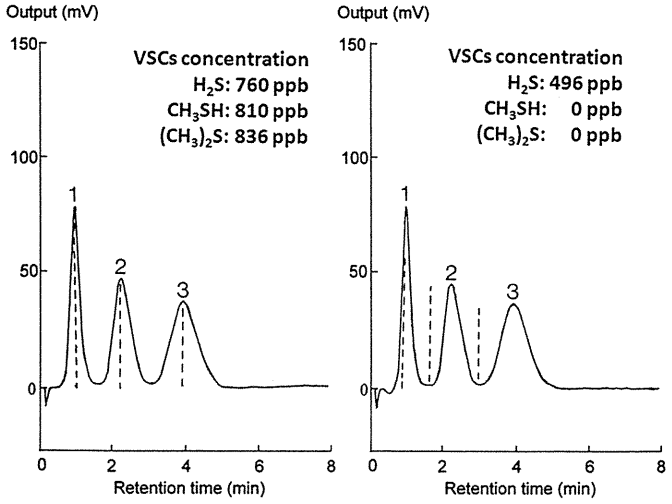

Figure 7. OralChroma™ chromatograms of a standard mixture of 1000 ppb each of H_2S, CH_3SH, and $(CH_3)_2S$ using a modified protocol [27]. Injection: 0.5 ml. The vertical dotted lines represent the assignments by OralChroma™ of H_2S, CH_3SH, and $(CH_3)_2S$. Left panel: correct assignment by OralChroma. Right panel: incorrect assignment by OralChroma. Peak assignment: 1 = H_2S, 2 = CH_3SH, 3 = $(CH_3)_2S$.

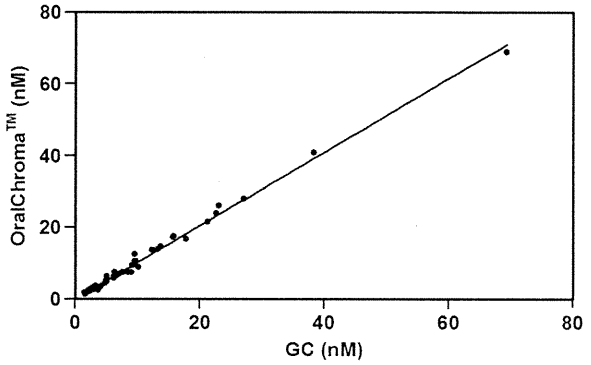

Figure 8. Comparison of the $(CH_3)_2S$ concentrations in mouth air obtained from the OralChroma™ using a modified protocol [27] with those obtained by a GC. Since no significant correlation was found between OralChroma display readings and GC measurements (figure 6(*C*)), $(CH_3)_2S$ concentrations obtained using a modified protocol were compared with GC results. Almost perfect correlation was found ($R = 0.997$, $y = 1.03x - 0.14$, $p < 0.0001$, $n = 55$).

$y = 0.95x$, $p < 0.0001$, $n = 137$) (figure 9(*B*)). For H_2S and CH_3SH measurements, the coefficients of determination were 0.94 and 0.81, respectively. Therefore, both measurements are reliable. The detection limit for H_2S was found to be 0.67 ng/10 ml.

Application of novel research protocols to clinical studies of $ZnCl_2$ products

The changes in VSC concentrations (ng/10 ml mouth air) are shown in figures 11 to 13. In total VSC concentrations, the use of zinc chloride mouthwash alone showed significant differences between the baseline and 0 h (immediately after treatment), 1 h, 2 h, and 3 h intervals post-treatment ($p < 0.001$, $p < 0.001$, $p < 0.005$, and $p < 0.01$, respectively) (see figure 10). For H_2S concentrations, significant differences were

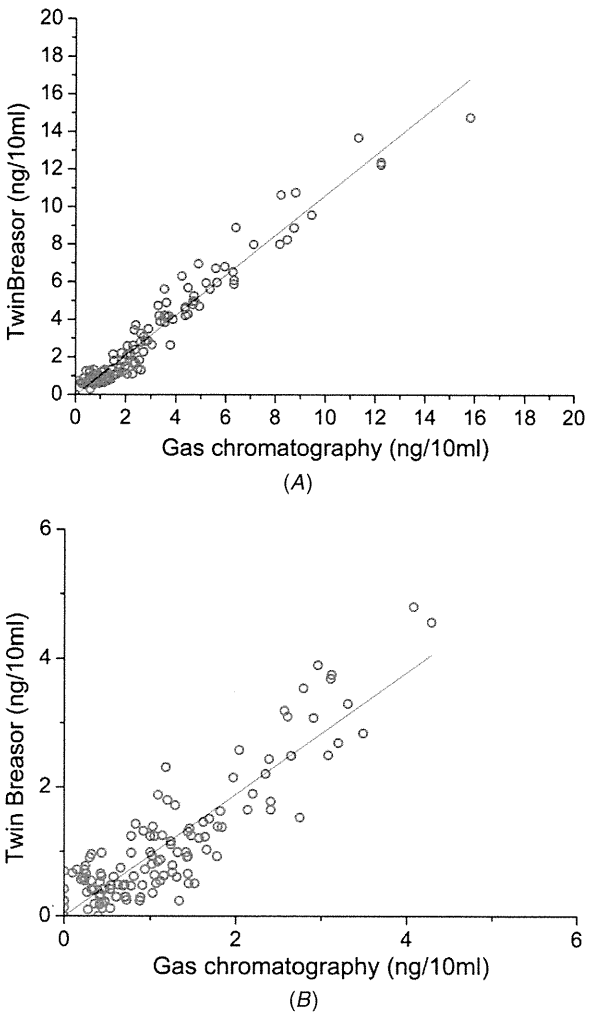

Figure 9. (*A*) Correlation between Twin Breasor™ display readings and GC measurements for H_2S. Significant correlation was found ($R = 0.97$, $y = 1.07x - 0.04$, $p < 0.0001$, $n = 137$). (*B*) Correlation between Twin Breasor™ display readings and GC measurements for CH_3SH. Significant correlation was found ($R = 0.90$, $y = 0.95x$, $p < 0.0001$, $n = 137$).

found between the baseline and 0 h, 1 h, 2 h, and 3 h intervals ($p < 0.001$, $p < 0.001$, $p < 0.005$, and $p < 0.01$, respectively) (figure 11). For CH_3SH concentrations, significant differences were found between the baseline and 0 h, 1 h, 2 h, and 3 h intervals ($p < 0.001$, $p < 0.001$, $p < 0.001$, and $p < 0.005$, respectively) (figure 12).

The combination treatment of tongue paste and mouthwash showed significant differences found between the baseline and 0 h, 1 h, 2 h, and 3 h intervals post-treatment for total VSC concentrations ($p < 0.001$, $p < 0.001$, $p < 0.01$, and $p < 0.05$, respectively) (figure 10). For H_2S concentrations, significant differences were found between the baseline and 0 h, 1 h, and 2 h intervals ($p < 0.001$, $p < 0.001$, and $p < 0.05$, respectively) (figure 11). For CH_3SH concentrations, the effects were the same as those demonstrated by the use of mouthwash alone.

The use of tongue paste alone also demonstrated significant differences in H_2S, CH_3SH and total VSC concentrations (ng/10 ml mouth air) immediately after the

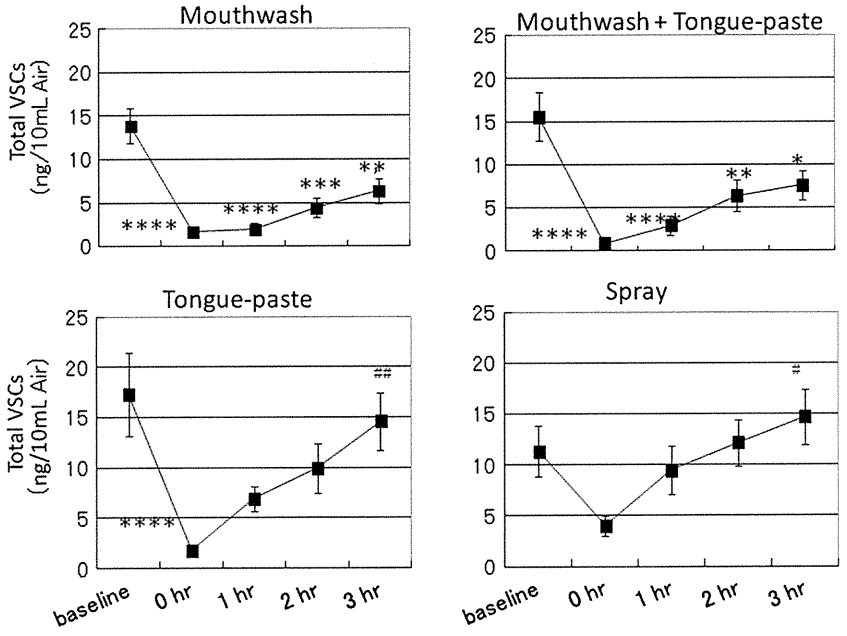

Figure 10. Percentage change in total VSC concentration. Both mouthwash alone and mouthwash and tongue paste combined showed similar significant differences at all measured time intervals. Tongue paste treatment reduced the concentration significantly at 0 h. Mouth spray demonstrated no significant difference between the baseline and other time intervals, although some reduction was found at 0 h. However, the reducing activity was significantly decreased at 3 h. ($^{*}p < 0.05$, $^{**}P < 0.01$, $^{***}p < 0.005$, and $^{****}p < 0.001$ between baseline and each time point; $^{\#}p < 0.05$ and $^{\#\#}P < 0.01$ between 0 h and 3 h [mean ± SE, $n = 10$].)

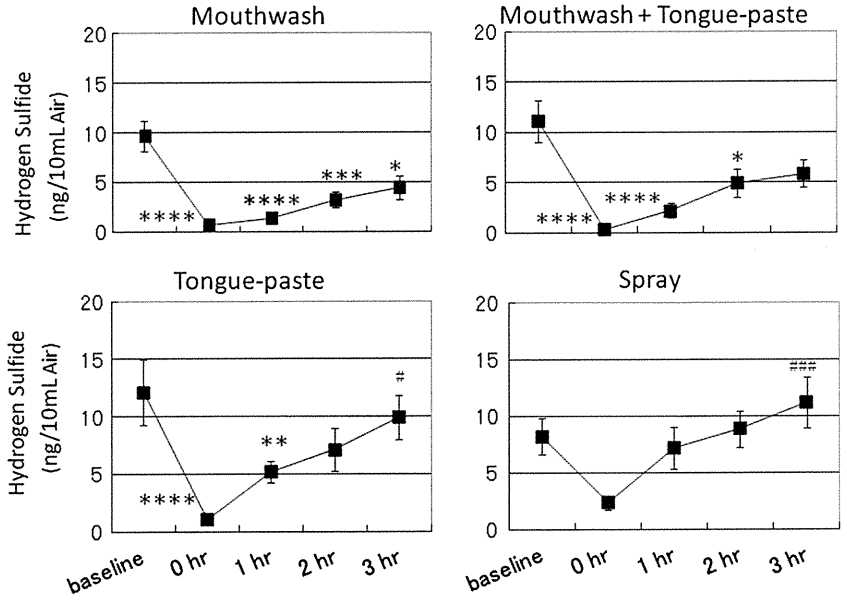

Figure 11. Percentage change in hydrogen sulfide concentration. Mouthwash alone and the combined treatment of tongue paste and mouthwash reduced the concentration significantly after the treatments. Tongue paste reduced the concentration significantly at 0 h and 1 h, but the reducing activity was completely lost at 3 h after the treatment. Mouth spray treatment showed no significant reduction in hydrogen sulfide concentration, but the reducing activity was significantly decreased at 3 h. ($^{*}p < 0.05$, $^{**}P < 0.01$, $^{***}p < 0.005$, $^{****}p < 0.001$, between baseline and each time interval; $^{\#}p < 0.05$ and $^{\#\#\#}P < 0.001$ between 0 h (immediately after treatment) and 3 h; mean ± SE, $n = 10$.)

treatments ($p < 0.001$, $p < 0.001$ and $p < 0.05$ respectively) (figures 11 to 13). Significant differences were also found between the baseline and the 1 h point in H_2S measurements (ng/10 ml mouth air) ($p < 0.01$) (figure 11). On the other hand, significant increments were also found between 0 h (immediately after treatment) and 3 h intervals in total VSC, H_2S and CH_3SH measurements (ng/10 ml mouth air) ($p < 0.01$, $p < 0.05$ and $p < 0.05$ respectively) for tongue paste alone. These results demonstrate the ineffectiveness of this treatment at 3 h after treatment (figures 11 to 12). However, spray alone did not demonstrate any significant reduction of VSCs.

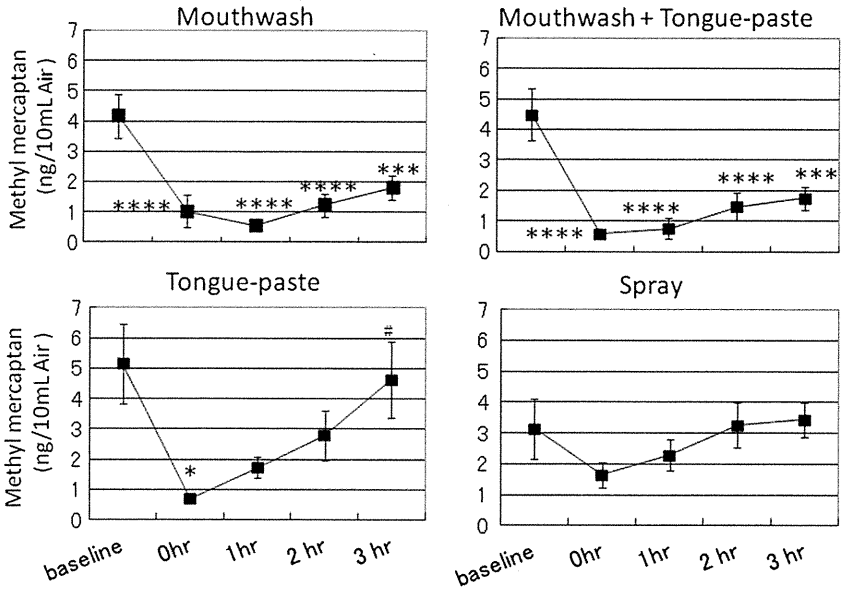

Figure 12. Percentage change in methyl mercaptan concentration. Mouthwash alone and mouthwash and tongue paste combined reduced the concentration significantly at all time intervals. Tongue paste reduced the concentration significantly at 0 h, but the reducing activity was significantly decreased at 3 h after the treatment. ($^{*}p < 0.05$, $^{**}P < 0.01$, $^{***}p < 0.005$, $^{****}p < 0.001$ between baseline and each time point; $^{\#}p < 0.05$ between 0 h (immediately after treatment) and 3 h; mean ± SE, $n = 10$.)

Discussion

This study demonstrates that a protocol combined with reliable GC instrumentation can be used to detect effects on oral malodor even when the baselines of the subjects vary. We found key factors for obtaining reliable results include the duration of the study, the time when measurements are made and limitations on the subjects' intake of food and fluids as well as oral hygiene procedures so that high baseline levels of VSC are available on which treatments can be tested.

For long-term clinical studies of halitosis it is often assumed that the baselines of VSCs or malodor are measured [11, 35, 38–40]. However, if the baseline of VSCs is not constant over several days or weeks, the premise of the research design is not tenable, and artifacts may be detected. We clearly demonstrated in this study that the baselines can fluctuate widely. No subject showed a constant VSC concentration at baseline during one week, even though measurements were made before the subjects were allowed to eat, drink, rinse or practice oral hygiene. Moreover, this baseline should be more constant than baselines measured later in the day, after subjects were allowed to eat.

The effects of menstruation in female subjects have been widely reported [42–44], and large fluctuations in VSCs at the baseline were found. However, based on human rights issues, ethics committees for clinical research can prohibit the elimination of females from the subject pool, and indeed, female subjects have been involved in many studies employing long-term protocol [11, 35, 38–40]. As a consequence, the assumption of constant baselines of VSCs or malodor is not valid and long-term clinical studies face problems of baseline variability. Instead, a short-term study of perhaps 3 h duration is recommended, as suggested by Tonzetich and Ng [45].

We determined the effect of eating meals on VSC concentration during a day. Our study clearly indicated that when the subjects refrained from eating, drinking and other oral-hygiene activities until lunchtime, they demonstrated the highest and most constant concentrations of VSCs in mouth air. However eating meals depresses VSC concentrations over 6 h after meals, as suggested by Tonzetich and Ng [45] or Fukui *et al* [36]. Existing guidelines, such as the Acceptance Program Guidelines established by the American Dental Association for products used in the management of oral malodor, allow the subjects to eat and drink until 4 h prior to evaluation of oral malodor [11]. Moreover, many study designs allowed their subjects to have meals up to a few or several hours prior to measurements [16, 46–49]. However, our study has clearly demonstrated that VSC concentrations drop dramatically immediately after a meal and then gradually increase until 6 h after the meal. Moreover, VSC concentrations at 6 h after a meal do not recover to the baseline level. It is strongly recommended that measurement of VSCs be carried out in the morning after the subject has refrained from eating, drinking, oral rinsing and oral-hygiene activity since midnight.

For oral malodor measurement, there are objective and subjective procedures. Organoleptic measurement is a subjective method [1, 2, 4, 5] making quantification of odor intensity notoriously difficult. In clinics a major problem of the organoleptic method is that it is impossible to ensure consistency in large numbers of judgments by several examiners. For calibrating and training the examiners, standard compounds (such as n-butanol) are utilized, but these compounds can not necessarily predict odor judges responses to VSCs [29, 50]. The primary contributors to oral malodor are H_2S and CH_3SH and these should be utilized for calibrating and training the examiners. In particular, various ratios of the mixtures as they exist in human mouth air must